Diatom, phytolith, and pollen records from a 10Be/9Be dated lacustrine succession in the Chad basin : insight on the Miocene–Pliocene paleoenvironmental changes in Central Africa

Alice Novello, Anne-Elisabeth Lebatard, Abderamane Moussa, Doris Barboni, Florence Sylvestre, Didier Bourles, Christine Paillès, Guillaume Buchet, Alain Decarreau, Philippe Duringer, et al.

Accepted manuscript now published in *Palaeogeography, Palaeoclimatology, Palaeoecology* (2015) 430: 85 - 103 〈10.1016/j.palaeo.2015.04.013〉

Diatom, phytolith, and pollen records from a $^{10}Be/^{9}Be$ dated lacustrine succession in the Chad basin: insight on the Miocene-Pliocene paleoenvironmental changes in Central Africa

Alice Novello[1, 2], Anne-Elisabeth Lebatard[2], Abderamane Moussa[3], Doris Barboni[2], Florence Sylvestre[2], Didier L. Bourlès[2], Christine Paillès[2], Guillaume Buchet[2], Alain Decarreau[4], Philippe Duringer[5], Jean-François Ghienne[5], Jean Maley[6], Jean-Charles Mazur[2], Claude Roquin[5], Mathieu Schuster[5], Patrick Vignaud[1]

[1] iPHEP, Institut de Paléoprimatologie, Paléontologie Humaine : Evolution et Paléoenvironnements, UMR 7262 CNRS-INEE - Université de Poitiers, 6 rue Michel Brunet, 86073 Poitiers Cedex 9, France

[2] Aix-Marseille Université, CNRS-IRD UM 34 CEREGE, Technopôle de l'Environnement Arbois-Méditerranée, BP80, 13545 Aix-en-Provence, France

[3] Département de Paléontologie, Université de N'Djamena, BP 1117, N'Djamena, Chad

[4] IC2MP, Institut de Chimie des Milieux et Matériaux de Poitiers, UMR 7285 CNRS - Université de Poitiers, 4 rue Michel Brunet - TSA 51106, 86073 Poitiers Cedex 9, France

[5] Institut de Physique du Globe de Strasbourg, UMR7516, CNRS - Université de Strasbourg/EOST, 1 rue Blessig, 67084 Strasbourg Cedex, France

[6] IRD & Département Paléoenvironnements, Institut des Sciences de l'Evolution de Montpellier, UMR 5554 CNRS, Université de Montpellier II, 34095, Montpellier, Cedex 5, France

*Corresponding author: A. Novello, Email: novelloalice@gmail.com

Abstract

A discontinuous 200m-long borehole drilled in the Bol Archipelago (13°N, Lake Chad) provided 25 samples which were dated with the $^{10}Be/^{9}Be$ method and analyzed for their micro-biological content. The dating provided ages ranging from 6.3±0.1 to 2.6±0.1 Ma, a period contemporaneous to the Pliocene fossil localities located in the current Chadian Djurab desert (16-17°N).

Well-preserved diatom assemblages first occurred at 4.7±0.1 Ma and remain dominated by the freshwater planktonic genera *Aulacoseira* and *Stephanodiscus* until the end of the Pliocene. This supports the recurrences of lacustrine conditions at Bol during all the Pliocene. The presence of pelite and argillaceous deposits in the core before 4.7±0.1 Ma, however, suggests that the lake settled earlier, at least since 6.3±0.1 Ma. The abundance of Afromontane pollen taxa at 4.2 ±0.1 Ma and the occurrence of trapeziform polylobate phytoliths throughout the sequence suggest significant vegetation inputs from the southern highlands. The importance of kaolinite in the clay sediments also indicates that a water supply predominantly from the south already existed at that time.

Phytolith assemblages are all dominated by lobate grass silica short cells and by blocky and elongate types, which attest to the presence of herbaceous-dominated vegetation around Bol and/or in the southern drainage basin during the Pliocene. This result is also supported with the pollen assemblage described at 4.2±0.1 Ma, which shows highest affinity for the savanna biome. Moreover, low values for the Xerophytic grass phytolith index indicate the presence of mesophytic grass communities in this vegetation.

Significant variations in the abundance of blocky and elongate phytoliths suggest local alternations of fully lacustrine and marshy conditions at Bol. Particularly between 3.6 and 2.7 Ma the abundance of silicified bulliform cells associated with the absence of diatoms support the hypothesis of a significant lacustrine reduction at Bol favoring the increasing of local marshy vegetation.

Keywords: Lake Chad, Sahara-Sahel, Miocene-Pliocene, vegetation, climate, hominin

Accepted manuscript now published in *Palaeogeography, Palaeoclimatology, Palaeoecology* (2015) 430: 85 - 103〈10.1016/j.palaeo.2015.04.013〉

1 Introduction

First hominins appeared during the late Neogene, when significant vegetation changes occurred in Africa (e.g. Bonnefille, 2010). These changes notably include the appearance and expansion of C_4 grasses (Cerling et al., 1997; Feakins et al., 2005; Edwards et al., 2010; Cerling et al., 2011; Strömberg, 2011; Dupont et al., 2013; Feakins et al., 2013), which are currently part of tropical grasslands and savannas at low altitude (Sage, 2004). Moreover, marine records off the African coasts indicate high climate variability in tropical Africa during the late Neogene (Feakins and deMenocal, 2010). This environmental variability is revealed by a succession of humid and arid phases tuned with precessional cyclicity of the Earth's orbit (deMenocal, 2004). Global vegetation and climate changes may have triggered hominin speciation and adaptive features (see review by Maslin et al., 2015). Particularly, the spread of C_4 grass savannas may have triggered the appearance of bipedalism in early hominins (e.g. Bonnefille, 2010; Cerling et al., 2011; Dominguez-Rodrigo, 2014). Among the factors that may have contributed to the increase of C_4 grasses in African landscapes, there is the decrease in the length but the intensification of the rainy season, or so called seasonality (Beerling and Osborne, 2006), and the subsequent enhancement of the fire activity (Archibald et al., 2009). Hydrological changes and the decrease of pCO_2 recorded at the end of the Miocene (Pagani et al., 1999) may also have been significant in the spread of C_4 plants in the African vegetation (Tipple and Pagani, 2010). As the hominin record is remarkably well documented in the East African rift system, much attention was given to this region for reconstructing late Neogene paleoenvironmental changes and especially C_4-grass expansion in Africa (Bonnefille, 2010). Indeed, about ten early hominin species from this region were described between the Messinian and the early Pleistocene, including three of the first hominins: *Orrorin tugenensis* (Kenya, ca 6 Ma, Senut et al., 2001), *Ardipithecus kaddaba, and Aridipithecus ramidus* (Ethiopia, ca 5.5-4.4 Ma, White et al., 1994; Haile-Selassie, 2001), and most of Australopithecines (Brown et al., 2013). The volcanic context of the East African rift system offers the advantage of providing datable ash layers useful for intersite paleoenvironmental comparisons. Biomarker data from the marine record DSDP231 off the East African coast indicate two major and distinct steps in the expansion of C_4 biomass in East Africa: one during the Tortonian (11-9 Ma) and one during the Pliocene (4.3-1.4 Ma) (Feakins et al., 2013). Yet the increase in C_4 biomass was not necessarily linked with an expansion of C_4 grasses but rather with a greater abundance of Amaranthaceae and Chenopodiaceae (xerophytic C_4 forbs) in the vegetation as precised by pollen data from the same record (Bonnefille, 2010).

In Chad (Central Africa), the hominin record is less documented than in the East African rift system but nevertheless significant. It includes *Sahelanthropus tchadensis* and *Australopithecus bahrelghazali*, which are the only two hominin species described in tropical Africa outside the East African rift valley (Brunet et al., 2002; Vignaud et al., 2002; Brunet et al., 2005). *S. tchadensis* is what's more the oldest hominin species described so far (Brunet et al., 2002). Fossil faunal assemblages associated with the Chadian hominins bear ages around 7 Ma for *S. tchadensis* and of 3.5 Ma for *A. bahrelghazali*, respectively (Brunet et al., 1995; Vignaud et al., 2002). The authigenic $^{10}Be/^{9}Be$ dating method applied to the fossiliferous areas of northern Chad produced after absolute ages that were consistent with the ages provided by faunas (Lebatard et al., 2008; Lebatard et al., 2010).

Paleoenvironmental studies at Chadian hominin sites (faunal composition and structure, dental mesowear and isotopes) concluded to the existence of a diversified vegetation cover, with a mosaic of forests, woodlands, grasslands, up to desert conditions, in close relationship with aquatic/lacustrine areas in northern Chad during the Messinian (Vignaud et al., 2002; Schuster et al., 2006; Jacques, 2007; LeFur et al., 2009; Schuster et al., 2009; Blondel et al., 2010; Otero et al., 2010), and open C_4-vegetations later on during the Pliocene (Brunet et al., 1997; Zazzo et al., 2000; Geraads et al., 2001; Lee-Thorp et al., 2012), in association with large lake occurrences (Schuster et al., 2009).

Paleovegetation modeling for the Messinian does not support the existence of mosaic

vegetation in northern Chad, but rather a spread of the tropical savanna biome (Pound et al., 2012). For the same time period for comparison, it suggests the simultaneous presence of tropical forests, savannas, and grasslands in eastern Africa (Pound et al., 2012). The apparent inconsistency between paleontological data and simulated biomes in northern Chad during the Messinian could be reconciled by considering that the recurring of large lake episodes must have triggered and sustained, at a local scale, dense and diverse riparian vegetation. Besides, the vegetation signal represented by fossil faunas from northern Chad may better reflect local environmental features related to lake littoral coasts and associated marsh/fluvial areas than regional biome. For the Pliocene period, vegetation modeling indicates that tropical savanna and/or xerophytic shrubland biomes were present in northern Chad (Salzmann et al., 2008; Contoux et al., 2013), which is consistent with the occurrence of C_4-dominated vegetation inferred from mammalian isotopic data (Zazzo et al., 2000; Lee-Thorp et al., 2012). Coupled climate-vegetation simulations also suggested that lacustrine episodes, even large, had little effect on biome distribution. During the mid-Pliocene, savanna and/or shrubland environments are therefore thought to result from regional climatic conditions rather than from lacustrine expansion (Contoux et al., 2013).

Paleobotanical data from the Lake Chad basin are restricted to the vertebrate localities of northern Chad. They consist of sparse silicified plant macro-remains (Coppens and Koeniguer, 1976) and abundant phytolith remains (Novello, 2012)preserved in paleosols, which are also full of fossilized root-systems and termite nests (Schuster et al., 2000; Duringer et al., 2006; Duringer et al., 2007) The identification of this termite nest suggests the presence of dry grasslands or more probably wooded savannas in northern Chad during the Miocene-Pliocene (Duringer et al., 2006).

Because previous paleoenvironmental investigations focused in the northern Lake Chad basin, more data from the southern Lake Chad Basin are needed to provide direct evidences for the presence (or not) of the savanna biome at the scale of all the Lake Chad basin, at time crucial for hominin emergence. In order to better document paleovegetation and paleohydrological changes that occurred in this part of the basin, we undertook the analysis of an old archive obtained in 1973 from the drilling of a borehole, at the locality of Bol (13°N). The drilling was carried out by the BRGM ("Bureau de Recherches Géologiques et Minières", France) during a campaign engaged for groundwater prospection in the Lake Chad basin. The samples (cuttings), since then kept by one of the co-authors (J. Maley), are now curated by l'Ecole et Observatoire des Sciences de la Terre (EOST, University of Strasbourg). We have first established the chronological background of this sedimentary archive by the determination of 25 new absolute ages using the authigenic $^{10}Be/^{9}Be$ dating method. We have then analyzed several micro-biological remains (phytoliths, pollen, and diatoms), which cover a time interval from about the Messinian (late Miocene) through the Piacenzian (late Pliocene). The results presented here are unique for both the time period and the place investigated.

2 Study area

The Lake Chad basin is a vast intracratonic basin of 2,500,000km², which expands on Chad, Niger, Nigeria, and Cameroon. It is bordered by the Tibesti uplift in the north (>3000m), the Ennedi and the Ouaddaï Plateaus in the east, the Adamaoua and Jos Plateaus in the south, and the Aïr and the Hoggar in the west. The basin consists of Cretaceous to Neogene deposits resting on a Paleozoic sedimentary cover and Proterozoic basement (Genik, 1992; Kusnir and Moutaye, 1997). The Neogene continental deposits mainly outcrop in the northern part of the Chadian basin (Schneider, 1989), in the Djurab desert, and consist in sequences of eolian sands and perilacustrine clayish sandstones interbedded with lacustrine mudstones and diatomites, the whole testifying of recurring large lake expansions in the region since at least 7 Ma (Vignaud et al., 2002; Schuster et al., 2006; Schuster et al., 2009). Four main Neogene fossiliferous areas are described in the Djurab according to their respective ages, sedimentary features, and faunal assemblages: TM (7.3±0.1 Ma, which yielded *Sahelanthropus tchadensis* fossil remains, KB (5.4±0.6 Ma), KL (4.0±0.1 Ma), and KT (3.6±0.1 Ma, which yielded *Australopithecus bahrelghazali* fossil remains (Brunet et al., 1995; Brunet et al., 1996; Brunet et al., 1998; Brunet and M.P.F.T., 2000; Brunet

et al., 2002; Vignaud et al., 2002; Brunet et al., 2005; Lebatard et al., 2010).

Present-day Lake Chad is supplied at 95% by the Chari-Logone river system, which drains a large basin of 620 000km² in the humid tropics from Central African Republic and North Cameroon, and to a lesser extent by direct rainfall and inflow from other small tributaries (El Beid and Komadugu Yobe rivers) (Bader et al., 2011; Leblanc et al., 2011). It is set in the Sahelian domain where mean annual rainfall is <400mm/yr, and dry season lasts from 9 to 11 months (Griffiths, 1972; New et al., 2002, CRU 10'x10' database). Average annual temperature is around 27-29°C (New et al., 2002).

The borehole of Bol (13°28'N, 14°44'E) was drilled in the southern part of the Lake Chad basin, at the edge of the Saharan desert, about 400 km to the south of the Miocene-Pliocene hominin localities (Fig.1). Bol is currently an archipelago surrounded by a large complex of small episodic islands of eolian sand, probably deposited in the region during the last glacial maximum (between 20-12 ka BP) (Servant, 1973). Present-day vegetation of Bol archipelago is essentially aquatic, with abundant herbaceous plants and few trees and shrubs (Gaston and Dulieu, 1976; Gaston, 1996; Olivry et al., 1996; César and Lebrun, 2003). Three vegetation types can be distinguished according to their distribution. (1) Aquatic areas are mostly occupied by hydrophytic Poaceae (grasses) (*Vossia cuspidata*, *Phragmites australis*, *Echinochloa* sp.), Cyperaceae (sedges) (*Cyperus papyrus, Cyperus articulatus)* and Typhaceae (*Typha domingensis*), which often constitute patches of vegetation drifting on water. The hydrophytic species *Aeschynomene elaphroxylon,* growing close to water courses and lake banks, may constitute dense vegetated areas when lake level is low (Gaston and Dulieu, 1976). (2) In areas that are regularly flooded and unflooded, the vegetation is mainly composed by marsh herbaceous taxa, such as Cyperaceae, *Potamogeton*, and hydro-/helophytic Poaceae (e.g. *Leersia hexandra*). (3) In contrast, drought-adapted plants, such as the shrub *Cassia sieberdana,* and xerophytic Poaceae such as *Cenchrus biflorus*, *Dactyloctenium aegyptium*, and *Panicum laetum* occur in the dry and sandy areas on the islands. On the highest islands, sub-desertic trees of *Acacia* sp., *Balanites aegyptiaca, Calotropis procera, Leptadenia pyrotechnica*, and Arecaceae (palm) trees of *Hyphaene thebaica* are also present.

3 Material

The sedimentary archive consists of a discontinuous succession of samples that could be originally associated with three major lithological units: alternating sand and clay at the bottom (673-297.2m), intermediate lacustrine pelite and diatomite (297.2-71.5m), and eolian sand at the top (71.5-0m) (Fig.2a) (Moussa, 2010). However, only 114 samples from the intermediate section between 297.2m and 71.5m were preserved. Of these, 25 samples (sampled between 297.2m and 90.8m) were studied as a test. These 25 samples were analyzed for $^{10}Be/^{9}Be$ dating, phytolith, pollen, and diatom remains. A supplementary sample, BOL 74 (74 m), was considered for $^{10}Be/^{9}Be$ dating only.

4 Methods

4.1 Dating

It has been demonstrated (Lebatard et al., 2008) that the environmental context prevailing since at least 8 Ma in the Chad basin is favourable for the use of the dating method based on the authigenic $^{10}Be/^{9}Be$ ratio (authigenic ^{9}Be isotope being used as a normalizing factor to overcome environmental effects (authigenic ^{9}Be isotope being used as a normalizing factor to overcome environmental effects, see Bourlès et al., 1989). This method offers the opportunity to date this 230m long sedimentary record.

The dating method applied here exactly follows the methodology used in Lebatard et al. (2008; 2010) for the Chadian hominin sites dating. Authigenic beryllium isotopes were selectively extracted from dried and crushed sediments using a 0.04M NH_2OH-HCl in a 25% acetic acid leaching solution (Bourlès et al., 1989). A 2ml aliquot is removed from the leachate for the ^{9}Be measurements. For the ^{10}Be measurements, the remaining leachate was spiked with 300µl of a 10^{-3} $g.g^{-1}$ ^{9}Be solution (Merck 1000mg/L Be standard), purified by solvent extractions of Be acetylacetonate in presence of EDTA followed by precipitations of $Be(OH)_2$ at pH 8.5 and rinsing. The final precipitate, dissolved in 100µl of HNO_3, is dried and heated at 800°C to obtain BeO. This chemical process and the measuring protocols were described in full details by

Lebatard and coll. (Lebatard et al., 2010 and references therein).

The study was conducted in two stages. The first six samples (BOL 74, 17h, 21j, 25a, 27n, and 32a; Table 1) ^{10}Be concentrations were measured at the now closed AMS Tandetron facility (Gif/Yvette, France), the ^{9}Be concentrations being measured on an Hitachi Z-8200 Atomic Absorption Spectrophotometer using Zeeman Effect background correction at CEREGE (Aix-en-Provence, France) as fully described in Ménabréaz et al. (2011). The 20 additional samples (Table 1) ^{10}Be concentrations were measured at the French AMS national facility ASTER installed since 2006 at CEREGE, the ^{9}Be concentrations being measured on a Thermo Scientific ICE 340 Atomic Absorption Spectrophotometer using Zeeman Effect background correction at CEREGE (Aix-en-Provence, France) as fully described in Lebatard et al. (2008; 2010). The ^{10}Be concentrations are normalized to ^{10}Be/^{9}Be SRM 4325 NIST reference material with an assigned value of $(2.79\pm0.03).10^{-11}$ (Nishiizumi et al., 2007). This standardization is equivalent to 07KNSTD within rounding uncertainty. The ^{10}Be half-life of $(1.39\pm0.01).10^{6}$ a (Chmeleff et al., 2010; Korschinek et al., 2010) was used for the age calculations, and the age uncertainties (1σ) result from the propagation of the ^{10}Be (linked to the number of ^{10}Be events detected coupled to a 3% analytical uncertainty deduced from the reproducibility through the measurement sequences), ^{9}Be and half-life uncertainties ultimately. ^{10}Be and ^{9}Be concentrations, the ^{10}Be/^{9}Be ratio and ^{10}Be/^{9}Be age of each individual sample are reported in Table 1.

4.2 Diatom, phytolith and pollen analyses

4.2.1 Laboratory procedures

Diatom analyses were conducted on 0-5g samples and treated through standard procedures (1:1 mixture of H_2O_2/water, 1:1 mixture of HCl/water, and repeatedly rinsed in distilled water; slides were made using Naphrax high resolution mounting) (Battarbee et al., 2001). For each sample, at least 400 diatom valves were identified and counted using a Nikon Eclipse 80i light microscope (differential interference contrast optics, x1000 magnification, N.A.=1.25). Specimens were identified to their lowest taxonomic level (i.e. variety) following the species concept used by Krammer and Lange-Bertalot (1986, 1988, 1991). However, many genera and species outlined have been re-assessed using the classification by Round et al. (1990) and synonyms are introduced. We quantified the number of diatom valves for each sample using an inverted microscope Olympus CKX41 following the procedure described by Fröhlich and Servant-Vildary (1989) (Table 2, Fig.2c). The concentration of diatoms is calculated using the dry weight of the sample and its dilution as well as the amount of dilution from which the diatom valve are numerated.

Phytolith analyses were conducted on 15g samples. Chemical treatment included carbonate dissolution with hydrochloric acid (HCl 37%), oxidation of organic matter with hydrogen peroxide (H_2O_2 33%, at 90°C), iron removal (with $C_6H_5Na_3O_7$ and $Na_2O_4S_2$, H_2O_2), clay removal by decantation, and densimetric separation with zinc bromide heavy liquid ($ZnBr_2$) set at d=2.3. The recovered silicified particles include phytoliths, diatoms, and sponge spicules. Glycerin was used as mounting medium to allow three-dimensional observations (WoldeGabriel et al., 2009). Silicified particles were counted at x400 and x1000 magnification. A minimum of 200 grass silica short cell phytoliths (GSSCs) was counted in each sediment sample, except for samples 30j, 26a, 21a and 9e for which the extracted material was exhausted before reaching the count. In these cases, only 143 to 192 GSSCs could be counted (Table S1). We estimated the relative abundances (%) of phytoliths, diatoms, and sponge spicules in each sample through counting of the silicified particles under the microscope (Table 2, Fig.2d). Phytoliths were classified following the classification criteria established by Novello et al. (2012) based on modern plants and soils from Chad. Photographs of phytoliths (Fig.3) were realized using Canada balsam as mounting medium because its refraction index (1.55) gives a better contrast than glycerin.

Pollen extraction was done using 5g of material and following the standard method of acid/base treatments. Carbonate-rich samples were treated with HCl (37%) before silicate removal using HF (40%, overnight), and humic acid removal using KOH (20%). Slides were mounted with glycerin. Pollen identifications

were performed at x1000 magnification. Only one (sample 25j) out of 25 samples contained enough pollen material for carrying out a suitable counting (total pollen sum of 803 grains, Table S2).

4.2.2 Modern phytolith reference data and analytical approaches

A modern soil/mud phytolith dataset of 57 surface samples from Chad (between 8°55'-13°56'N and 15°33'-20°06'E) was used as a reference for interpreting the phytolith signal of fossil sediments from Bol. The modern dataset includes samples from the marshes of current Lake Chad (10) and from various Sahelian (18) and Sudanian (29) environments and savanna types (Novello, 2012; Novello et al., 2012). Sixteen phytolith soil samples from the Guineo-Congolian forests (Runge, 1999) were also included in our modern referential where grass-dominated environments are obviously over-represented.

The D/P° index (Bremond et al., 2008), which is the ratio of tree and shrub phytoliths (i.e. globular granulate types) over grass (Poaceae) phytoliths (grass silica short cells exclusively) was used as a proxy for the openness of the environment (Fig.4). Globular echinate phytoliths (not included in the D/P° index) were used to infer the presence of the Arecaceae family, i.e. palms (Barboni et al., 2010; Albert et al., 2014). The relative abundance of blocky and elongate phytoliths was used to trace lacustrine marshes, following our observations of modern surface soil samples (Fig.4). Indeed, although blocky and elongate phytoliths may have various origins (trees, shrubs or herbaceous taxa) (e.g. Strömberg, 2003; Mercader et al., 2009), we observed that they are more abundant in the surface samples of current Lake Chad marshes and of Sahelian temporary swamps than in any other surface soil samples of the sub-Saharan region (Novello et al., 2012). Among the blocky types, we gave particular attention to the cuneiform (fan-shaped) phytoliths. These are produced in the bulliform cells, of grasses and sedges (Novello et al., 2012). Heavy silicification of bulliform cells occurs when these plants undergo high evapotranspiration rate while their root system is submerged (Sangster and Parry, 1969). Indeed, silicified bulliform cells happen to be particularly abundant in mud samples from current sub-Saharan marshes (Fig.4) (Novello, 2012). We used the Aquatic and Xerophytic grass phytolith indices (hereafter Iaq and Ixe) (Novello et al., 2012) now calibrated on an extended modern plant dataset of 98 grass species (Novello, 2012) as proxies for the environmental affinity of grass communities (Fig.4). Based on the new calibration, Iaq and Ixe phytolith indices are defined as follows,

$$\mathbf{Iaq} = \frac{Ro2 + Ro6 + Bi7 + Bi11 + Bi12 + Cr3 + Cr5 + Cr6 + Cr7 + Bi14 + Poly1}{N_{tot\ GSSC}} \text{ X } 100$$

$$\mathbf{Ixe} = \frac{Ro1 + Ro5 + Bi2 + Bi3 + Bi4 + Bi15 + S1 + S2 + S3}{N_{tot\ GSSC}} \text{ X } 100$$

Where $N_{tot\ GSSC}$ is the total of GSSC types counted for each sample, Ro: Rondel, Bi: Bilobate, Cr: Cross, S: Saddle (see Novello, 2012 for morphological details of the phytolith types used in the indices).

When applied to modern soil/mud surface assemblages, the newly calibrated grass phytolith indices provide a better identification of herbaceous wetland marshes, and of grasslands of the Sahelian and Sudanian domains than the indices calibrated previously on a smaller grass dataset (Novello et al 2012) (Figure S1). The Ixe index was here preferred to the Iph index (Bremond et al., 2005b) because it intends to exclude the phytolith signal of local aquatic grasses. The abundance of aquatic grasses on the lake margins may indeed conceal the phytolith signal of extra-local (i.e. non lacustrine) grass communities more representative of the regional vegetation.

Decision trees (rpart function, R.13.0) based on modern phytolith assemblages were used to produce threshold values of the Iaq and of the Ixe indices, below and above which a fossil sample can be related to the Sudanian, Sahelian, or Lake Chad (aquatic) grass signal. Above an Iaq index value of 34%, most phytolith assemblages are related to Lake Chad marshes (8/9 assemblages, 89% of accurate classifications). Below this threshold value of 34% for Iaq, phytolith assemblages are unlikely to originate from aquatic environments but rather from surrounding grass communities of the Sahelian or Sudanian domains (Fig.4, Fig.7). A threshold value of 46% for the Ixe index allows discriminating Sudanian phytolith assemblages from Sahelian phytolith assemblages (Fig.4, Fig.7). As a result, most

modern Sahelian phytolith assemblages (15/18 assemblages, 83% of accurate classifications) have Ixe index values ≥46%. We are aware that the robustness of these thresholds and indices is criticized, as it depends on the number of phytoliths taken in account for calculating the grass phytolith indices Iaq and Ixe (here ranging from 33 to 114 phytoliths) (Strömberg, 2009). These thresholds were therefore used as a support to reflect the main tendencies recorded in the fossil phytolith assemblages.

4.2.3 Modern pollen reference data and analytical approaches

The biomization method was applied to the pollen sample 25j (Jolly et al., 1998). Biome scores (%) were calculated for the fossil pollen data of Bol, and compared to scores calculated from modern pollen data of Lake Chad (Maley, 1972, 1981; Amaral et al., 2013). Score values were obtained from pollen abundance data (square-root transformed to lower the weight of over-represented taxa) and from known taxa ecological and phytogeographical affinities (Fig.8). Assignment of pollen taxa to pant functional types (PFTs) and of PFTs to biomes follow Lézine et al. (2009) (Appendix 2).

5-Results

5.1 $^{10}Be/^{9}Be$ ages

Twenty-five authigenic $^{10}Be/^{9}Be$ ratios were measured. Using the initial ratio N_0 of $(2.54\pm0.09).10^{-8}$ determined from Holocene diatomites of Megalake Chad (~7 to 4.4 ka BP) (Schuster et al., 2005; Lebatard et al., 2008) and the ^{10}Be decay period of $(1.387\pm0.012).10^{6}$ years (Chmeleff et al., 2010; Korschinek et al., 2010), the resulting authigenic $^{10}Be/^{9}Be$ ages range from 6.35±0.11 Ma at the bottom (at 297.2m depth) to 2.61±0.08 Ma for the top sample (at 90.8m depth). The Bol sequence therefore represents a time interval from the Messinian (late Miocene) to the Piacenzian (late Pliocene) (Table 1). A sedimentation rate of about 53.0m.Ma^{-1} was estimated from linear regression performed with initial age data (Fig.5). The upper sample BOL 74 (Table 1) corresponding to 74m of depth yields an authigenic $^{10}Be/^{9}Be$ ratio similar to the initial ratio N_0 of $(2.54\pm0.09).10^{-8}$ (Lebatard et al., 2008). This initial ratio is used here, because it was established using specifically selected diatomites deposited during the last Holocene expansion of Megalake Chad (~7 to 4.4 ka BP). Lacustrine diatoms built their silica skeleton made from dissolved nutrients and thus are an ideal substrate for registering the dissolved isotopic ratio of $^{10}Be/^{9}Be$ at the time they were alive (Lebatard et al., 2008).

We obtained eight date inversions along the chronological sequence. An age-model was therefore calculated in order to represent the fossil abundances along a time scale (Fig.5). This model excludes the upper sample BOL 74 related to late Pleistocene times. Each modeled age value was estimated from the linear equation defined by the age values of its closest neighboring samples. This method was also used to provide absolute ages for the non-dated samples (24n and 32a) (Table 1). A linear regression performed from age model values provides a new estimated sedimentation rate value of about 54.5m.Ma^{-1} (Fig.5). We consider our age model reliable because it barely changes the sedimentation rate estimated from initial data (53.0m.Ma^{-1}).

5.2 Diatom, phytolith, pollen remains

5.2.1 Occurrences, preservation, and relative abundance

Of the 25 analyzed samples, four are sub-sterile in diatoms and phytoliths, five only sub-sterile in diatoms, and two sub-sterile in phytoliths (Table 2). Sub-sterile samples 35e, 35a, 32e, and 32a are part of the oldest section of the record and dated to >5.6 Ma. They include <5µm non-describable bio-silica fragments, as well as sparse and very fragmented diatom frustules. Other samples sub-sterile in diatoms are dated to 5.5±0.1 Ma (30j) and between 3.6±0.1 and 2.5±0.1 Ma (17a, 13e, 11a, and 8n). Samples sub-sterile in phytoliths are dated to 4.4±0.1 Ma (27n) and 2.4±0.1 Ma (6p). We note that fragmentation (and dissolution?) of phytoliths and/or diatoms is common also in the samples rich in bio-silica particles (Fig.3).

The number of diatom valves in the sediment is highly variable as concentrations range from 1.10^{7} valves/g of dry sediments to $>18.10^{6}$ valves/g of dry sediments (Table 2, Fig.2c). The relative abundance of phytoliths (versus diatoms and sponge spicules) ranges from 0 to 100% (Fig.2d). Out of 21 samples, 17 are dominated by phytoliths. Particularly during the 3.6±0.1 to 2.4±0.1 Ma time interval, phytoliths account for >61% of the siliceous particles

5.2.2 Diatom assemblages

The diatom-rich samples are dominated by two freshwater planktonic genera: *Aulacoseira* and *Stephanodiscus* (Table 2). *Aulacoseira granulata* (Ehrenberg) Simonsen is the dominant species, accounting for >50% in all sample, and up to 90% in samples 27n, 22a, 21a, 10b, and 6p. The occurrence of *Stephanodiscus carconensis* Grunow and its varieties is limited to the time interval between 4.3±0.1 and 2.5±0.1 Ma (samples 26a to 9e). *S. carconensis* accounts for up to 37% of the total diatom assemblages with two major peaks of abundance in samples 26a (4.3±0.1 Ma) and 17h (3.6±0.1 Ma) (Table 2, Fig.6).

Other diatom species account for 1% to 30% and include a variety of both planktonic (such as *Cyclotella* spp., *Coscinodiscus* spp.) and epiphytic species (such as *Navicula confervacea* (Kützing) Grunow, *Nitzschia compressa* (Bailey) C. S. Boyer, and *Rhopalodia gibba* (her.) O. Müller) (Table S1). Epiphytic diatoms are rare: they occur in 11 out of 16 samples and represent<5% (Table 2). Sample 28a (4.7±0.1 Ma), which has the highest diatom valves concentration, also exhibits the highest diatom diversity with a total of 23 species, against an average of nine species in other samples (Table 2). In this sample, epiphytic diatoms account for 4%.

5.2.3 Phytolith assemblages

We observed 40 different types of grass silica short cells (GSSCs) and 25 non-GSSC types (Table S1). Among these, two types of trapeziform polylobate phytoliths (Poly3 and Poly4) were not observed in modern soil/sediment assemblages of Chad (Novello et al., 2012). Poly3 type is characterized by an irregular and narrow multi-lobate base topped by a rectangular to keeled top that can reach up to 20µm in height (Fig.3, 13). Poly4, on the contrary, has a regular multi-lobate base topped by a well-defined rectangular top that does not exceed 8µm in height (Fig.3, 14).

GSSCs, blocky bodies and elongates are the most abundant phytolith categories present in the fossil samples. GSSCs (Poaceae) account for 18-82% of the total assemblages, while blocky and elongate types (ubiquists) account for 2-55% and 4-29%, respectively (Table 2). When present, globular phytoliths (mostly related to trees, shrubs, and palms) account for <14%, Cyperaceae papillae and Commelinaceae polyhedral phytoliths for ≤1% of the total phytolith assemblages (Table 2). Among the GSSCs (Poaceae), the lobate phytolith types (bilobates, crosses, and tabular polylobates) are most abundant and represent 61% to 94% of the total GSSC assemblages. Rondel and saddle phytolith types are less represented as they account for <28% and <13% of the GSSC assemblages, respectively. Polylobate trapeziform GSSCs (Poly3, Poly4) are observed in 7 out of 19 samples but represent <2% of the total GSSC assemblages (Table 2).

The D/P° ("Dicot versus Poaceae phytoliths") index is strictly <0.1 for all 25 samples between 5.5±0.1 and 2.4±0.1 Ma (Table 2, Fig.6). Such low D/P° values are observed for present-day grass-dominated environments of the Sudanian and Sahelian domains. They are strikingly different from the D/P° values of >2.5 obtained for the climatic forests of the Guineo-Congolian domain (Fig.6). Arecaceae (palms) phytoliths are rare in all samples except 30j (5.5±0.1 Ma) where they reach 13% of the total phytolith assemblage (Fig.6). The (ubiquist) blocky and elongate phytoliths are present in remarkable amounts (29-38%) between 3.6±0.1 and 3.2±0.1 Ma (Fig.6). Such abundances are observed in modern sediment samples from current marshes near Lake Chad (Fig.6). Peaks of abundance of silicified bulliform cells are recorded at 3.6±0.1, 3.4±0.1, and 3.2±0.1 Ma (38%, 17%, and 29%, respectively). Abundances of silicified bulliform cells >17% are associated, in our modern referential (Novello et al., 2012), with samples from Lake Chad marshes only. The Ixe index strictly <41% suggests fossil grass communities with mesic preferences in the regional vegetation (Fig.6, Fig.7). For seven samples (28a, 25j, 24n, 21a, 13e, 11a, and 9e), the Iaq index signal is >38% and therefore close to that of aquatic grasses that may have been present in the local vegetation associated with the lake (Fig.6, Fig.7). For other samples the Iaq is ≤35%, and therefore also remains close to that of regional mesophytic grass communities (Fig.6, Fig.7).

5.2.4 Pollen assemblage (sample 25j)

The only productive sample for pollen analysis (25j, 4.2±0.1 Ma) is characterized by abundant Poaceae (68%) and Cyperaceae (15%) elements, and the marked presence of about a total of 7% of tree taxa leaving today only in the

southern reach of the Chad basin (Table S2). These southern pollen taxa belong to Guineo-Congolian elements (<1%) with *Tetrorchidium*, to Sudano-Guinean elements (3%) with *Alchornea* (3%), *Acalypha, Hymenocardia,* and *Syzygium guineense*, and to Afromontane elements (4%) with *Olea capensis* (4%), *Maesa, Myrica,* and *Rapanea melanophloeos* (Table S2).

Biome scores calculated for sample 25j are highest for SAVA (savanna) and STEP (steppe) (Fig.8). Moreover, they are higher for the WAMF (warm afromontane forest), TSFO (tropical seasonal forest), and TRFO (tropical rain forest) biomes in comparison with present-day and Holocene biome scores also obtained from Lake Chad area (after Maley, 1972, 1981; Amaral et al., 2013) (Fig.8).

6 Discussion

More than 100 samples from the Bol borehole were available to us but just the 25 samples for which we obtained $^{10}Be/^{9}Be$ authigenic dating were chosen for micro-botanical analyses. The resulting dataset is therefore a partial contribution that could be further improved to document paleoenvironmental changes that occurred in the Lake Chad Basin during the Miocene-Pliocene. Nevertheless, our study provides the first paleoenvironmental data set that is directly comparable with other coeval records in continental Africa because each sample has an absolute age (Salzmann et al., 2008; Bonnefille, 2010; Feakins et al., 2013) thus providing direct evidences of paleovegetation and paleohydrological conditions in Central Africa Chad basin between 6 and 2 Ma.

6.1 Diatom biostratigraphy and absolute $^{10}Be/^{9}Be$ ages

The Bol diatom record is consistent with the known biostratigraphy of *Stephanodiscus carconensis* Grunow in the fossil lacustrine records from Africa (Gasse, 1980) (Fig.6). *S. carconensis* seems to have appeared during the late Miocene of Africa, diversified during the Pliocene, and finally disappeared during the early Pleistocene (Gasse and Fourtanier, 1991). As no diatoms were preserved in the Bol record before 4.7 Ma, the first appearance of *S. carconensis* during the late Miocene cannot be confirmed here. Higher abundance of *S. carconensis* and higher number of varieties between 4.7±0.1 and 3.6±0.1 Ma support a Pliocene diversification. After 2.7±0.1 Ma, *S. carconensis* only accounts for <1%, while other species as *Stephanodiscus medius* Häkansson and *Stephanodiscus astraea* (Ehrenberg) Grunow make their apparition and diversify (Table S1). This pattern may be interpreted as a sign of *S. carconensis* disappearance at the beginning of the Pleistocene. The agreement between the *S. carconensis* occurrence time span and the calculated $^{10}Be/^{9}Be$ ages along the core section, in which the species is present, confirms the reliability of the dating method based on meteoric ^{10}Be (Lebatard et al., 2008; Lebatard et al., 2010). *Stephanodiscus carconensis* varieties occurred in Africa during the Messinian and reached their optimal development in large lakes during the Piacenzian (Gasse and Fourtanier, 1991). At that time, they were widespread throughout the world (Gasse and Fourtanier, 1991). In the Afar region (Ethiopia), for instance, where at least three successive lacustrine phases occurred between 2.5 and 0.75 Ma, they predominate before 1.5 Ma (Gasse, 1980).They disappeared from the African continent during the early Pleistocene, but still survive today in some great temperate lakes of the Northern Hemisphere. Their disappearance from the African continent is assumed to result from the establishment of arid conditions which prevailed during the middle Pleistocene, and which led to desiccation of the northern African large lakes (Servant-Vildary, 1978; Gasse and Fourtanier, 1991).

6.2 The paleo-lake Chad: evidence and variations during the Miocene-Pliocene

Diatom assemblages dominated by *Aulacoseira granulata* and *Stephanodiscus carconensis* support freshwater lacustrine conditions at Bol (even interrupted) 4.7±0.1 Ma. *Aulacoseira* and *Stephanodiscus* are considered as freshwater planktonic species. They were widespread during the Piacenzian and early Pleistocene in large and deep lakes from East Africa (Gasse, 1980, 1986), the Chad basin (Servant, 1973), and the Hoggar (Rognon, 1967). *Aulacoseira granulata* still dominates the present-day diatom flora, notably in Lake Chad (Rirongarti, 2014). The core lithology between 297m and 230m, and below 297m depth, however, suggests that lacustrine sedimentation most likely occurred earlier than the first diatom

evidence recorded at 4.7±0.1 Ma, probably as early as 6.3±0.1 Ma (Fig.2). Indeed, before 4.7±0.1 Ma, the Bol sequence includes pelites (35a, 35e), sandy claystones (32a), and apparently argillaceous "diatomite" (32e, 30j) according to the macroscopic aspect of sediments. Microscopic investigations of the sediments dated older than 5.5±0.1 Ma, however, revealed no preserved diatoms (or phytoliths) but <5µm non-describable bio-silica fragments (35e, 35a, 32e, and 32a). These fragments may be related to undetermined diagenetic processes had affected the preservation of bio-silica material (including both diatoms and phytoliths) in this part of the core. It is not possible, therefore, to document paleoenvironmental changes and lake variations at Bol before 5.5 Ma although the nature of sediments attests to the presence of a lake.

Sample 30j, dated to 5.5±0.1 Ma, provides the oldest biogenic evidence. It has no diatoms but is rich in phytoliths of obligate terrestrial plants such as palm trees. In this sample, palm phytolith abundance (about 13%) is comparable to that observed in modern soil samples from the Sudanian and Sahelian domains (Fig.6). Elsewhere in the Bol sequence, the abundance of palm phytoliths never exceeds 5%. This suggests that terrestrial vegetation was present in the close surroundings of Bol around 5.5 Ma, just at the end of the Messinian, and that peri-lacustrine condition may therefore have prevailed at Bol during that time. During the Pliocene, the dominance of planktonic *Aulacoseira* species indicates the existence of expanded water areas at Bol. At 4.7±0.1 Ma, the diatom flora is remarkably diversified and abundant (Table 2), as it can be observed during a lacustrine expansion. After 4.7±0.1 Ma and then until 2.4±0.1 Ma, variations in the abundance of diatom frustules (per gram of sediments) then suggest successive phases of expansion-regression of the lake, or otherwise *in-situ* modifications of the lake properties that would have prevented the optimal development of diatoms. Extreme water turbidity as well as low silica availability, which is most unlikely in the Lake Chad basin (Olivry et al., 1996), may impede an optimal development of diatoms. But as the aquatic grass phytolith signal also varies temporally during that period (Fig.6), it is likely that alternating marshy and fully lacustrine conditions occurred at Bol during the Pliocene as it did during the Holocene (Maley, 1977; Maley, 1980, 2010). At 4.4±0.1 Ma (27n) and 2.4±0.1 Ma (6p), no phytoliths and pollen, but only diatoms are observed. This may indicate fully lacustrine conditions at Bol, with lake margins located too far to allow any phytolith input from plants. It is unlikely that post-depositional dissolution of phytoliths occurred, given the great preservation of diatoms in these sediments. Phytolith preservation may have been altered during transport from the (local and regional) sources to the lake, but it would then be surprising that they all suffered similarly from total dissolution at all these different original places and/or during transport along their different journey.

After ~3.6 Ma (17h), the quasi-absence of diatoms likely suggests (episodic or continuous?) reduced lacustrine conditions at Bol until at least 2.7±0.1 Ma (10b), which are consistent with high abundances of blocky-elongate phytoliths (including silicified bulliform cells) recorded in the same sediments (Fig.6, Table 2). In modern sub-Saharan environments of Chad, blocky-elongate phytoliths, and notably silicified bulliform cells, are most abundant in wetland sediments from marshes where aquatic herbaceous vegetation is dominant (Novello et al., 2012). High relative abundances of silicified bulliform cells only may be related to plants with submerged root system undergoing high evapotranspiration rates (Novello et al., 2012). Combined evidences of marshy vegetation and high evapotranspiration rates at the same time interval suggest a temporary period of increased aridity in the Lake Chad basin. This hypothesis is consistent with a general trend toward aridification in the basin from ~7 Ma to 3 Ma inferred from oxygen isotopes on fish remains from northern Chad (Otero et al., 2011). Lake variations recorded at Bol are also in agreement with repeated lacustrine transgressive events documented in northern Chad (>16°N) during the Pliocene (Schuster et al., 2009).

6.3 A lake supplied from the south

Several botanical and sedimentary evidences suggest that major water input to paleolake Chad came from its southern drainage basin. Fluvial contributions from the south are first inferred from the pollen assemblage at 4.2±0.1 Ma. Maley (1972, 1981) previously showed that the presence of taxa living in the humid south (Sudano-Guinean, Guineo-Congolian zones) in

modern pollen assemblages of Lake Chad, clearly indicates that these pollens were brought by fluviatile influx. Such a pattern was also suggested for Holocene sediments originated from the Kanem region, in the north-east of Lake Chad (Maley, 2004). Moreover, the Pliocene pollen assemblage is also rich in southern Afromontane pollen taxa such as *Olea capensis, Rapanea melanophloeos, Maesa,* and *Myrica*. These taxa only occurs nowadays in the Adamawa and Jos plateau, which are located at mid-elevation and close to the southern reach of the Chad Basin (Letouzey, 1968). For instance, similar pollen taxa were determined for a middle Holocene pollen spectrum obtained on a core collected in Lake Mbalang (7°19'N, 13°44'E, 1110m a.s.l.), located in the eastern Adamawa plateau (Vincens et al., 2010). Conversely, taxa from the northern Saharan uplifts such as the olive tree *Olea europea* (Letouzey, 1968) are totally absent in the Pliocene pollen assemblage. Water supply from the south is also consistent with the presence of kaolinite in the clay fraction (Moussa, 2010). Kaolinite is the main clay mineral developed in lateritic weathering profiles of the tropical zone. It has been identified as the preponderant mineral in the suspended matter presently exported from their southern catchment by the Logone and Chari rivers to the lake (Gac, 1980; Gac and Tardy, 1980; Olivry et al., 1996).

Compared to biome scores calculated for modern and Holocene pollen assemblages from sediments of Lake Chad (Maley, 1972, 1981; Amaral et al., 2013), the WAMF (warm afromontane forest) biome score is significantly higher at 4.2±0.1 Ma. This may also suggest a more intense drainage of the southern highlands than observed nowadays. The occurrence of trapeziform polylobate phytoliths related to C_3-Pooideae grasses (Barboni and Bremond, 2009; Rossouw, 2009) throughout the Bol sequence also further supports this hypothesis. Indeed, these types are currently absent in modern phytolith assemblages of the Lake Chad basin (Novello et al., 2012).

6.4 Tropical savanna as the dominant biome

Both phytolith and pollen data from the Bol sequence are congruent with the presence of the savanna biome during the Miocene-Pliocene in the Lake Chad basin. Low D/P° index values (<<1) and high relative abundance of grass pollen (68%) are indeed typical for savannas and grasslands. The Ixe phytolith index suggests that humid-preference but likely non-lacustrine grasses, i.e. mesophytic grasses, occurred in the Lake Chad basin during all the Pliocene. The Iaq phytolith index indicates that local aquatic grasses contributed to the grass phytolith signal recorded at Bol. It is noteworthy that no significant xerophytic grass signal is indicated by the Ixe phytolith index (Fig. 6, Fig.7), even during the period of increased aridity that we hypothesized to have settled between 3.6 and 2.7±0.1 Ma. The absence of xerophytic grass signal in the phytolith record is even more surprising considering the high steppe biome score that we obtained for the pollen assemblage at 4.2±0.1 Ma (Fig.8). Thus we expect that the grass phytolith inputs to the lake during the Pliocene were quasi-exclusively originated from fluvial contributions from the humid south and from the local grasslands associated with the lake.

Climate and hydrological simulations for the mid-Pliocene (with fixed CO_2 at 405ppm) show three potential biomes in the Lake Chad basin: tropical xerophytic shrubland, tropical savanna, and tropical deciduous forest/woodland (Salzmann et al., 2008; Contoux et al., 2013). The most forested biome (tropical deciduous forest/woodland) is simulated when the ITCZ reaches a northerly position (Contoux et al., 2013). The phytolith and pollen grass signals support the presence of the tropical savanna biome in the Lake Chad basin as far as the Bol locality throughout the Pliocene, and therefore give poor support for the existence of tropical xerophytic shrubland for latitudes <13°N. As the savanna biome was present, the monsoon regime probably reached a more northern position during the summer rainfall season than observed nowadays in Central Africa, but not far enough to allow forest biome to expand until the location of Bol. Forest tropical biomes, therefore, were most likely present in the southern part of the drainage basin of paleolake Chad during the Pliocene, as suggested by higher biome scores for tropical seasonal and rain forests at 4.2±0.1 Ma than for modern and Holocene samples (Fig.8).

The presence of the tropical savanna biome at 13°N does not exclude abundant ligneous taxa in the paleovegetation, as it is observed for some modern savannas ("woodland savanna", "tree savanna", Boughey, 1957). Phytoliths are

good indicators to trace the existence of true tropical forest environments in tropical Africa (Fig.4) (Bremond et al., 2005a; Aleman et al., 2011) but, conversely, they still fail to reconstruct the ligneous cover in tropical savanna environments (Neumann et al., 2009; Novello et al., 2012), As a result, these present phytolith data cannot provide much information on the presence/abundance of the ligneous cover in these paleo-savannas. The abundance of globular decorated phytoliths, as well as the values of the D/P° phytolith index observed for fossil samples, could be only indicative of a >2m-ligneous cover ranging from 0% to 80% according to the calibration performed between our modern phytolith data and ligneous cover percentages directly estimated at the modern Chadian sites we sampled (Fig.9). Then the existence of savannas with high ligneous component cannot be totally excluded since Aleman et al. (2014) also have demonstrated that the "super-local" grassy vegetation associated with a lake may hide the signal from the surroundings and regional vegetation.

6.5 Lesson for the Pliocene grass expansion in Central Africa

Evidences of grass-dominated vegetation are observed in northern Chad (16°N) during the Messinian (Blondel et al., 2010), but it is likely that the spread of grass-dominated environments occurred by the Zanclean-Piacenzian boundary, around 3.6 Ma (Zazzo et al., 2000; Geraads et al., 2001)Our data cannot document the history of grasses in Central Africa before ~5.5 Ma as no micro-botanical remains were preserved in the Bol core beyond this period. However, our data suggest that the expansion of grasses in Central Africa may have occurred earlier than the Zanclean as grass silica short cell phytoliths already account for 61% in Bol sediments around the Miocene-Pliocene boundary (at ~5.5 Ma). This is also consistent with the increase of grass cuticles and pollen grains recorded in a core off the Niger Delta (5-6°N) during the Messinian, just before the Miocene-Pliocene transition (Morley and Richards, 1993). Carbonate isotopes on mammalian teeth (including the hominin *Australopithecus bahrelghazali*) indicate that C_4 vegetation was dominant in northern Chad (16°N) around 3.6 Ma (Zazzo et al., 2000; Lee-Thorp et al., 2012). At Bol, the fossil assemblages are dominated by bilobate, cross (i.e. lobate), and saddle phytoliths (Table 2; Fig.6), which are most likely related to C_4 grasses according to previous phytolith studies (Fredlund and Tieszen, 1994; Barboni et al., 1999; Bremond et al., 2005b; Bremond et al., 2008)

Recent studies, however, have demonstrated that some lobate and saddle phytoliths may also be produced by C_3 aquatic grass species. This was notably observed for the C_3 aquatic species *Phragmites australis* (Arundinoideae), which can produce about 68% of saddle phytoliths in its leaves, and for the C_3 aquatic species *Leersia hexandra* (Ehrhartoideae), which can produce 21% of lobate (bilobate, cross, and tabular polylobate) phytoliths in its leaves (Novello et al., 2012). Today, these aquatic grass species are part of the aquatic herbaceous vegetation present in the Lake Chad marshes, and therefore are expected to largely contribute to the phytolith assemblages of modern sediments deposited in the lake. However, C_3 aquatic grasses cannot presently be properly identified using phytoliths. *Phragmites*, for instance, produces trapeziform saddles that are not identified to the genus-level (Novello et al., 2012) because they can be confused with trapeziform saddles also produced by some tropical C_4 grass species of the Chloridoideae subfamily such as *Cynodon dactylon* and *Eragrostis pilosa* (Fig.9), and even of the Panicoideae subfamily such as *Andropogon gayanus* (Fig.9) currently occurring in the Lake Chad basin (Gaston, 1996). A similar ambiguity applies to *Leersia hexandra*. This species produces indeed various types of lobate phytolith types (Bi2, Bi8, Bi11, and Poly11) that can be also produced by tropical C_4 grass species of the Aristidoideae subfamily such as *Aristida stipoides* (Fig.9), and of the Panicoideae subfamily such as *Andropogon pseudapricus, Diheteropogon amplectens,* and *Panicum laetum*) (Fig.9) currently occurring in the Lake Chad basin (Gaston, 1996). Some authors (Neumann et al., 2009; Prasad et al., 2011), however, asserted to have identified a specific bilobate type – "the bilobate type with scoped ends" – which they described as diagnostic of the Ehrhartoideae grass subfamily. The description criteria and classification used in this study were not designed to specifically isolate this bilobate type that may have thus be counted as part of the bilobate types with notched ends (Bi8 type) (see Table 3 for Bi-8 photograph), which in fact

probably include a larger morphological variability than the bilobate type with scoped ends itself. Although a new counting of the fossil samples of Bol should be done to investigate the presence of this diagnostic type in the record, further investigations are nevertheless needed to allow discriminating C_3 aquatic grasses from C_4 grasses using phytoliths. The respective presence/abundance of C_3 and C_4 grasses in the Bol area during the Pliocene thus remains still uncertain.

6.6 New insight on climate in Central Africa during the Pliocene

The Pliocene is known to include long periods of warmer and cooler climate than today (Feakins and deMenocal, 2010). The mid-Pliocene is particularly characterized by higher global mean annual temperatures (+2-3°C) (Ravelo et al., 2004) compared to present times (Feakins and deMenocal, 2010; Salzmann et al., 2011; Contoux et al., 2012). At Bol, the mid-Pliocene global warm event may be expressed by an aridification of the climate as suggested by the paucity of diatom remains, and the abundance of marsh phytolith indicators (blocky and elongate phytoliths), and high evapotranspiration rates (silicified bulliform cells). Besides it is likely that North, West, and Central African regions all experienced aridity during the mid-Pliocene. Indeed, pollen records indicate aridification of the northwestern African climate between ~3.5 and ~3.2 Ma, and at ~2.8 Ma (Leroy and Dupont, 1994, 1997), while dust records from marine core indicate increased wind strength at ~2.8 Ma in West Africa (deMenocal, 2004). Mid-Pliocene aridity may be related to significant elevated *p*CO2 (330-425ppm) compared to present times (200-260ppm) (Pagani et al., 2010), and/or to direct effects of Northern Hemisphere Glaciation such as ocean circulation and trade wind modification (Feakins and deMenocal, 2010; Salzmann et al., 2011).

6.7 Pliocene environment and hominin occurrences in tropical Africa

Finally the core sediments provide no micro-biological remains during the time spanning Sahelanthropus tchadensis occurrence. During Abel's occurrence (~3.6 Ma) major changes in the micro-biological record occurred at Bol, interpreted as a lake regression under higher arid climate conditions. For the same period in the Djurab (further north), evidences of C4 vegetation (Lee-Thorp et al., 2012), open environments (Zazzo et al., 2000; Geraads et al., 2001), and trend toward aridity (Otero et al., 2011) were observed. In East Africa, the early occurrence of Australopithecus afarensis is also dated from ~3.6 Ma at Laetoli in Tanzania (White, 1985). Phytoliths from Laetoli beds indicate a shift to xeric environmental conditions followed by an increase of C4 grasses in the vegetation (Rossouw and Scott, 2011), which is similar to the signal recorded in the Lake Chad basin for the same time interval. A trend toward aridity, in relationship with a Chenopodiaceae and Amaranthaceae pollen increase, has also been recorded at the regional scale in East Africa around 3.6 Ma (Bonnefille, 2010). Yet it seems that arid conditions have not impeded the presence of hominins in both Central and East Africa during the Zanclean-Piacenzian boundary. Such arid conditions may have notably favored the evolution of hominins in Africa through bipedalism, which may allow them consuming less energy under high-temperature conditions (Wheeler, 1991a, b).

7 Conclusion

The study of the Bol borehole provides new evidences on the paleoenvironment that prevailed in the Lake Chad basin during the Miocene-Pliocene, between c.a. 6 and 2 Ma. The nature of the sedimentation indicates that Paleo-Lake Chad existed at least since 6.3±0.1 Ma, but probably settled earlier during the Miocene (Moussa, 2010). Siliceous remains are however too poorly preserved to document the lacustrine conditions and the surrounding vegetation that existed at Bol before 5.5±0.1 Ma. Both sedimentology (for instance. kaolinite in the sediments) and plant remains (presence of Afromontane pollen taxa, and occurrence of C_3-Pooideae phytolith types) are consistent with the hypothesis that water supply to the lake during the Pliocene originated from the southern regions, including the southern highlands. Preserved diatom floras and phytolith assemblages attest for fully lacustrine conditions in the southern Lake Chad Basin during the beginning of the Zanclean (4.7-4.1±0.1 Ma) and at the end of the Piacenzian (2.7-2.4±0.1 Ma), and peri-lacustrine conditions at the end of the Messinian (at 5.5±0.1 Ma) and during the beginning of the Piacenzian (3.6-2.7±0.1 Ma). Phytolith assemblages and pollen elements indicate the presence of the tropical savanna biome in the

Lake Chad basin during the Pliocene, in agreement with previous simulations by models (Salzmann et al., 2008; Salzmann et al., 2011; Coutoux, 2013). Another important result only observed between 3.6 and 2.7±0.1 Ma, is that sediment diatom concentration exhibits a significant decrease, concomitantly with the increase of blocky and elongate phytoliths, including the silicified bulliform cells, in the phytolith assemblages. This evidence supports the aridification recorded in northern Chad and elsewhere in North and West Africa during the Zanclean-Piacenzian transition (Leroy and Dupont, 1994, 1997; Otero et al., 2011).

The first question that arises concerns the paleoenvironmental conditions that existed at Bol before the Zanclean. The second question concerns the respective role of C_3 and C_4 grasses in the region in relationship with aquatic vegetated areas. Only the analyses of additional fossil samples of the Bol record as well as a deep and continuous lacustrine record combined with advanced micro-biological remains calibrations on modern material would enable to complete this dataset. Moreover, further paleontological excavations regarding the Piacenzian deposits of northern Chad would confirm the hypothesis that the event recorded at Bol may have impacted the evolution of vertebrate faunas in the region, and particularly hominins.

Acknowledgments

This work was carried out as part of AN's doctoral research on phytoliths in Chad, with the financial support of the CNRS and the Région Poitou-Charentes. We thank the Chadian Authorities (Ministère de l'Education Nationale de l'Enseignement Supérieur et de la Recherche, University of Ndjamena, Centre National d'Appui à la Recherche), the Ministère Français de l'Enseignement Supérieur et de la Recherche (UFR SFA, University of Poitiers, INEE/CNRS, ANR, Project ANR-09-BLAN-0238, PI's M. Brunet), and the Ministère Français des Affaires Etrangères (DCSUR Paris and French Embassy in Ndjamena, Chad; FSP, Project no. 2005-54 of the Franco-Chadian cooperation) for financial support and permissions to conduct research in Chad. M. Arnold, G. Aumaître and K. Keddadouche are thanked for their valuable assistance in ^{10}Be measurements at the ASTER AMS national facility (CEREGE, Aix en Provence) which is supported by the INSU/CNRS, the ANR through the "Projets thématiques d'excellence" program for the "Equipements d'excellence" ASTER-CEREGE action, IRD and CEA. We thank A. Ducarre for his help in assessing diatom concentrations in the sediments as well as IRD for funding the diatom analysis, and P. Amaral for her help in providing her pollen data. This study would not have been possible without F. Humbert (EOST, Strasbourg) for preliminary lithological investigations on this core, and P. Poilecot (CIRAD, Montpellier), who largely contributed to the building of AN's modern phytolith dataset.

References

Albert, R.M., Bamford, M.K., Esteban, I., 2014. Reconstruction of ancient palm vegetation landscapes using a phytolith approach. Quaternary International (in press).

Aleman, J., Leys, B., Apema, R., Bentaleb, I., Dubois, M.A., Lamba, B., Lebamba, J., Martin, C., Ngomanda, A., Truc, L., Yangakola, J.-M., Favier, C., Bremond, L., 2011. Reconstructing savanna tree cover from pollen, phytoliths and stable carbon isotopes. Journal of Vegetation Science 23, 187-197.

Aleman, J.C., Canal-Subitani, S., Favier, C., Bremond, L., 2014. Influence of the local environment on lacustrine sedimentary phytolith records. Palaeogeography, Palaeoclimatology, Palaeoecology 414, 273-283.

Amaral, P.G.C., Vincens, A., Guiot, J., Buchet, G., Deschamps, P., Doumnang, J.-C., Sylvestre, F., 2013. Palynological evidence for gradual vegetation and climate changes during the African Humid Period termination at 13°N om a Mega-Lake Chad sedimentary sequence. Climate of the Past 9, 1-19.

Archibald, S., Roy, D.P., van Wilgen, B.W., Scholes, R.J., 2009. What limits fire? An examination of drivers of burnt area in Southern Africa Global Change Biology 15, 613-630.

Bader, J.-C., Lemoalle, J., Leblanc, M., 2011. Modèle hydrologique du Lac Tchad. Hydrological Sciences Journal 56, 411-425.

Barboni, D., Ashley, G.M., Dominguez-Rodrigo, M., Bunn, H.T., Mabulla, A.Z.P., Baquedano, E., 2010. Phytoliths infer locally dense and heterogeneous paleovegetation at

FLK North and surrounding localities during upper Bed I time, Olduvai Gorge, Tanzania. Quaternary Res 74, 344-354.

Barboni, D., Bonnefille, R., Alexandre, A., Meunier, J.D., 1999. Phytoliths as paleoenvironmental indicators, West Side Middle Awash Valley, Ethiopia. Palaeogeography, Palaeoclimatology, Palaeoecology 152, 87-100.

Barboni, D., Bremond, L., 2009. Phytoliths of East African grasses: An assessment of their environmental and taxonomic significance based on floristic data. Rev Palaeobot Palyno 158, 29-41.

Battarbee, R.W., Jones, V.J., Flower, R.J., Cameron, N.G., Bennion, H., 2001. Diatoms, in: Smol J. P., Birks H. J. B., M., L.W. (Eds.), Tracking Environmental Change using Lake Sediments. Kluwer Academic Publishers, The Netherlands, Dordrecht, pp. 155-202.

Beerling, D.J., Osborne, C.P., 2006. The origin of the savanna biome. Global Change Biology 12, 2023-2031.

Blondel, C., Merceron, G., Andossa, L., Taisso, M.H., Vignaud, P., Brunet, M., 2010. Dental mesowear analysis of the late Miocene Bovidae from Toros-Menalla (Chad) and early hominid habitats in Central Africa. Palaeogeography, Palaeoclimatology, Palaeoecology 292, 184-191

Bonnefille, R., 2010. Cenozoic vegetation, climate changes and hominid evolution in tropical Africa. Global and Planetary Change 72, 390-411.

Boughey, A.S., 1957. The physiognomic delimination of West African vegetation types. J W Afr Sci Ass 3, 148-165.

Bourlès, D.L., Raisbeck, G.M., Yiou, F., 1989. ^{10}Be and ^{9}Be in marine sediments and their potential for dating. Geochimica Cosmochimica Acta 53, 443-452.

Bremond, L., Alexandre, A., Hély, C., Guiot, J., 2005a. A phytolith index as a proxy of tree cover density in tropical areas: Calibration with Leaf Area Index along a forest–savanna transect in southeastern Cameroon. Global and Planetary Change 45, 277-293.

Bremond, L., Alexandre, A., Peyron, O., Guiot, J., 2005b. Grass water stress estimated from phytoliths in West Africa. Journal of Biogeography 32 311-327.

Bremond, L., Alexandre, A., Wooller, M.J., Hély, C., Williamson, D., Schäfer, P.A., Majule, A., Guiot, J., 2008. Phytolith indices as proxies of grass subfamilies on East African tropical mountains. Global and Planetary Change 61, 209-224.

Brown, F.H., McDougall, I., Gathogo, P.N., 2013. Age Ranges of *Australopithecus* Species, Kenya, Ethiopia, and Tanzania, in: Reed, K.E., Fleagle, J.G., Leakey, R.E. (Eds.), The Paleobiology of *Australopithecus*. Springer Netherlands, pp. 7-20.

Brunet, M., Beauvilain, A., Coppens, Y., Heintz, E., Moutaye, A.H.E., Pilbeam, D., 1995. The first australopithecine 2500 kilometres west of the Rift Valley (Chad). Nature 378, 273-275.

Brunet, M., Beauvilain, A., Geraads, D., Guy, F., Kasser, M., Mackaye, H.T., Maclatchy, L.M., Mouchelin, G., Sudre, J., Vignaud, P., 1998. Tchad : découverte d'une faune de mammifères du Pliocène inférieur. Comptes Rendus de l'Académie des Sciences de Paris 326, 153-158.

Brunet, M., Beauvilain, A., Geraads, D., Guy, F., M. Kasser, H.T., Mackaye, Maclatchy, M.L., Mouchelin, G., Sudre, J., Vignaud, P., 1996. *Australopithecus bahrelghazali*, une nouvelle espèce d'Hominidé ancien de la région de Koro Toro (Tchad). Comptes Rendus de l'Académie des Sciences de Paris Série IIa 322, 907-913.

Brunet, M., Geraads, D., Guy, F., Kasser, M., Mackaye, H.T., MacLatchy, L.M., Mouchelin, G., Sudre, J., Vignaud, P., 1997. Tchad: un nouveau site à Hominidés Pliocène. Comptes-Rendus de l'Académie des Sciences IIa 324, 341-345.

Brunet, M., Guy, F., Pilbeam, D., Lieberman, D.E., Likius, A., Mackaye, H.T., Léon, M.S.P.d., Zollikofer, C.P.E., Vignaud, P., 2005. New material of the earliest hominid from the Upper Miocene of Chad. Nature 434, 752-755.

Brunet, M., Guy, F., Pilbeam, D., Mackaye, H.T., Likius, A., Ahounta, D., Beauvilain, A., Blondel, C., Bocherensk, H., Boisserie, J.-R., Bonis, L.d., Y. Coppens, Dejax, J., Denys, C., Duringer, P., Eisenmann, V., Fanone, G., Fronty, P., Geraads, D., Lehmann, T., Lihoreau, F., Louchart, A., Mahamat, A., Merceron, G., Mouchelin, G., Otero, O., Pelaez-Campomanes, P., Leon, M.P.D., Rage, J.-C., Sapanetk, M., Schuster, M., Sudre, J., Tassy, P., Valentin, X., Vignaud, P., Viriot, L., Zazzo, A., Zollikofer,

C., 2002. A new hominid from the Upper Miocene of Chad, Central Africa. Nature 418, 145-151.

Brunet, M., M.P.F.T., 2000. Chad, discovery of a vertebrate fauna close to the mio-pliocene boundary. Journal of Vertebate Paleontology 20, 205-209.

Cerling, T.E., Harris, J.M., MacFadden, B.J., Leakey, M.G., Quade, J., Eisenmann, V., Ehleringer, J.R., 1997. Global vegetation change through the Miocene/Pliocene boundary. Nature 389, 153-158.

Cerling, T.E., Wynn, J.G., Andanje, S.A., Bird, M.I., Kimutai Korir, D., Levin, N.E., Mace, W., Macharia, A.N., Quade, J., Remien, C.H., 2011. Woody cover and hominin environments in the past 6 million years. Nature 476, 51-56.

César, J., Lebrun, J.-P., 2003. Flore du Tchad. Laboratoire de Recherches Vétérinaires et Zootechniques de Farcha, N'Djaména, p. 477.

Chmeleff, J., von Blanckenburg, F., Kossert, K., Jackob, D., 2010. Determination of the ^{10}Be half-life by multicollector ICP-MS and liquid scintillation counting. Nuclear Instruments and Methods in Physics Research B 268, 192-199.

Contoux, C., Jost, A., Ramstein, G., Sepulchre, P., Krinner, G., Schuster, M., 2013. Megalake Chad impact on climate and vegetation during the late Pliocene and the mid-Holocene. Climate of the Past 9, 1417-1430.

Contoux, C., Ramstein, G., Jost, A., 2012. Modelling the mid-Pliocene Warm Period climate with the IPSL coupled model and its atmospheric component LMDZ5A. Geoscientific Model Development 5, 903-917.

Coppens, Y., Koeniguer, J.C., 1976. Sur les flores ligneuses disparues Plio-Quaternaires du Tchad et du Niger. Comptes Rendus de l'Académie des Sciences de Paris 265, 1282-1285.

Coutoux, C., 2013. Megalake Chad impact on climate and vegetation during the late Pliocene and the mid-Holocene. Climate of the Past 9, 1417-1430.

deMenocal, P.B., 2004. African climate change and faunal evolution during the Pliocene-Pleistocene. Earth and Planetary Science 220, 3-24.

Dominguez-Rodrigo, M., 2014. Is the "Savanna Hypothesis" a Dead Concept for Explaining the Emergence of the Earliest Hominins? Current Anthropology 55, 59-81.

Dupont, L.M., Rommerskirchen, F., Mollenhauer, G., Schefuß, E., 2013. Miocene to Pliocene changes in South African hydrology and vegetation in relation to the expansion of C_4 plants. Earth and Planetary Science Letters 375, 408-417.

Duringer, P., Schuster, M., Genise, J.F., Likius, A., Mackaye, H.T., Vignaud, P., Brunet, M., 2006. The first fossil fungus gardens of Isoptera: oldest evidence of symbiotic termite fungiculture (Miocene, Chad basin). Naturwissenschaften 93, 610-615.

Duringer, P., Schuster, M., Genise, J.F., Mackaye, H.T., Vignaud, P., Brunet, M., 2007. New termite trace fossils: Galleries, nests and fungus combs from the Chad basin of Africa (Upper Miocene-Lower Pliocene). Palaeogeography, Palaeoclimatology, Palaeoecology 251, 323-353.

Edwards, E.J., Osborne, C.P., Strömberg, C.A.E., Smith, S.A., Consortium, C.G., 2010. The Origins of C_4 Grasslands: Integrating Evolutionary and Ecosystem Science. Science 328, 587-591.

Feakins, S.J., deMenocal, P.B., 2010. Global and African Regional Climate during the Cenozoic, in: Werdelin, L., Sanders, W. (Eds.), Cenozoic Mammals of Africa. , University of California Press.

Feakins, S.J., deMenocal, P.B., Eglinton, T.I., 2005. Biomarker records of late Neogene changes in northeast African vegetation. Geology 33, 977–980.

Feakins, S.J., Levin, N.E., Liddy, H.M., Sieracki, A., Eglinton, T.I., Bonnefille, R., 2013. Northeast African vegetation change over 12 m.y. Geology 41, 295-298.

Fredlund, G.G., Tieszen, L.T., 1994. Modern Phytolith Assemblages from the North American Great Plains. Journal of Biogeography 21, 321-335.

Fröhlich, F., Servant-Vildary, S., 1989. Evaluation of diatom content by counting and infrared analysis in Quaternary fluvio-lacustrine deposits from Bolivia. Diatom Research 4, 241-248.

Gac, J.Y., 1980. Géochimie du bassin du lac Tchad : Bilan de l'altération, de l'érosion et de la sédimentation, Travaux et documents de l'ORSTOM, p. 252.

Gac, J.Y., Tardy, Y., 1980. Géochimie d'un paysage tropical : le bassin du lac Tchad, in:

Tardy, Y. (Ed.), Géochimie des interactions entre les eaux, les minéraux et les roches. ARL Eléments, pp. 199-239.

Gasse, F., 1980. Les diatomées lacustres plio-pléistocènes du Gadeb (Ethiopie), Systématique, Paléoécologie, Biostratigraphie. Revue Algologique, p. 249.

Gasse, F., 1986. East African diatoms. Taxonomy, ecological distribution, Bibliotheca Diatomologica, p. 201.

Gasse, F., Fourtanier, E., 1991. African diatom paleoecology and biostratigraphy, in: Lang, J., Kobke, C.A. (Eds.), African Continental Sediments. Pergamon Press, Oxford.

Gaston, A., 1996. Agropastoralisme, in: CIRAD (Ed.), Atlas d'Elevage du Bassin du Lac Tchad. CTA, Waganingen, pp. 39-55.

Gaston, A., Dulieu, D., 1976. Pâturages naturels du Tchad. Département d'Elevage et Médecine Vétérinaire des Pays Tropicaux, Maison Alfort.

Genik, G.J., 1992. Regional framework, structural and petroleum aspects of rift basins in Niger, Chad and the Central African Republic (C.A.R.). Tectonophysics 213, 169-185.

Geraads, D., Brunet, M., Mackaye, H.T., Vignaud, P., 2001. Pliocene Bovidae (Mammalia) from the Koro Toro Australopithecine sites, Chad. Journal of Vertebrate Paleontology 21, 335-346.

Griffiths, J.F., 1972. General introduction, in: Griffiths, J.F. (Ed.), Climates of Africa. Elsevier, Amsterdam, p. 604.

Haile-Selassie, Y., 2001. Late Miocene hominids from the Middle Awash, Ethiopia. Nature 412, 178-181.

Jacques, L., 2007. Les préférences écologiques (paléorégimes alimentaires, paléohabitats) des grands mammifères herbivores des sites à hominidés du miocène supérieur du Nord Tchad. Reconstitution au moyen de l'analyse isotopique en carbone et oxygène du carbonate de l'émail dentaire, PhD Thesis. Université de Poitiers.

Jolly, D., Prentice, I.C., Bonnefille, R., Ballouche, A., Bengo, M., Brenac, P., Buchet, G., Burnet, D., Cazet, J.-P., Cheddadi, R., Edorh, T., Elenga, H., Elmoutaki, S., Guiot, J., Laarif, F., Lamb, H., Lézine, A.-M., Maley, J., Mbenza, M., Peyron, O., Reille, M., Reynaud-Farrera, I., Riollet, G., Ritchie, J.C., Roche, E., Scott, L., Ssemmanda, I., Straka, H., Umbr, M., Campo, E.V., Vilimumbalo, S., Vincens, A., Waller, M., 1998. Biome reconstruction from pollen and plant macrofossil data for Africa and the Arabian peninsula at 0 and 6000 years. Journal of Biogeography 25, 1007-1027.

Korschinek, G., Bergmaier, A., Faestermann, T., Gerstmann, U.C., Knie, K., Rugel, G., Wallner, A., Dillmann, I., Dollinger, G., Lierse von Gosstomski, C., Kossert, K., Maiti, M., Poutivtsev, M., Remmert, A., 2010. A new value for the ^{10}Be half-life by Heavy-Ion Elastic Recoil detection and liquid scintillation counting. . Nuclear Instruments and Methods in Physics Research B 268, 187-191.

Krammer, K., Lange-Bertalot, H., 1986. Süsswasserflora von Mitteleuropa. Bacillariophyceae. Teil 1: Naviculaceae, Jena.

Krammer, K., Lange-Bertalot, H., 1988. Süsswasserflora von Mitteleuropa. Bacillariophyceae. Teil 2: Bacillariaceae, Epithemiaceae, Surirellaceae, Jena.

Krammer, K., Lange-Bertalot, H., 1991. Süsswasserflora von Mitteleuropa. Bacillariophyceae. Teil 3: Centrales, Fragilariaceae, Eunotiaceae, Jena.

Kusnir, I., Moutaye, H.A., 1997. Resources minérales du Tchad: une revue. Journal of African Earth Sciences 24, 549-562.

Lebatard, A.-E., Bourlès, D.L., Braucher, R., Arnold, M., Duringer, P., Jolivet, M., Moussa, A., Deschamps, P., Roquin, C., Carcaillet, J., Schuster, M., Lihoreau, F., Likius, A., Mackaye, H.T., Vignaud, P., Brunet, M., 2010. Application of the authigenic ^{10}Be/^{9}Be dating method to continental sediments: Reconstruction of the Mio-Pleistocene sedimentary sequence in the early hominid fossiliferous areas of the northern Chad Basin. Earth and Planetary Science Letters 297, 57-70.

Lebatard, A.-E., Bourlès, D.L., Duringer, P., Jolivet, M., Braucher, R., Carcaillet, J., Schuster, M., Arnaud, N., Monié, P., Lihoreau, F., Likius, A., Mackaye, H.T., Vignaud, P., Brunet, M., 2008. Cosmogenic nuclide dating of *Sahelanthropus tchadensis* and *Australopithecus bahrelghazali*: Mio-Pliocene hominids from Chad. Proceedings of the National Academy of Sciences 105, 3226-3231.

Leblanc, M., Lemoalle, J., Bader, J.C., Tweed, S., Mofor, L., 2011. Thermal remote sensing of water under flooded vegetation: New

observations of inundation patterns for the 'Small' Lake Chad. Journal of Hydrology 404, 87-98.

Lee-Thorp, J., Likius, A., Mackaye, H.T., Vignaud, P., Sponheimer, M., Brunet, M., 2012. Isotopic evidence for an early shift to C4 resources by Pliocene hominins in Chad. Proceedings of the National Academy of Sciences 109, 20369-20372.

LeFur, S., Fara, E., Mackaye, H.T., Vignaud, P., Brunet, M., 2009. The mammal assemblage of the hominid site TM266 (Late Miocene, Chad Basin): ecological structure and paleoenvironmental implications. Naturwissenschaften 96, 565-574.

Leroy, S., Dupont, L., 1994. Development of vegetation and continental aridity in northwestern Africa during the Late Pliocene: the pollen record of ODP Site 658. Palaeogeography, Palaeoclimatology, Palaeoecology 109, 295-316.

Leroy, S., Dupont, L., 1997. Marine palynology of the ODP site 658 (N-W Africa) and its contribution to the stratigraphy of the Late Pliocene. Geobios 30, 351-359.

Letouzey, R., 1968. Etude phytogéographique du Cameroun, in: Lechevalier, P. (Ed.), Encyclopedia biologica n°69, Paris, p. 511.

Lézine, A.-M., Watrin, J., Vincens, A., Hély, C., 2009. Are modern pollen data representative of west African vegetation? Review of Palaeobotany and Palynology 156, 265-276.

Maley, J., 1972. La sédimentation pollinique actuelle dans la zone du lac Tchad (Afrique Centrale). Pollen et Spores 14, 263-307.

Maley, J., 1977. Palaeoclimates of Central Sahara during the early Holocene. Nature 269, 573-577.

Maley, J., 1980. Les changements climatiques de la fin du Tertiaire en Afrique: leur conséquence sur l'apparition du Sahara et de sa végétation, in: Williams, M.A.J., Faure, H. (Eds.), The Sahara and the Nile. A. A. Balkema, Rotterdam, pp. 63-86.

Maley, J., 1981. Etudes palynologiques dans le bassin du Tchad et paléoclimatologie de l'Afrique nord-tropicale de 30 000 ans à l'époque actuelle, PhD. Université de Montpellier, Travaux & Documents ORSTOM, n° 129, Paris.

Maley, J., 2004. Le bassin du Tchad au Quaternaire récent : formations sédimentaires, paléoenvironnements et préhistoire. La question des paléotchads., in: Sémah, A.-M., Renault-Miskovsky, J. (Eds.), L'évolution de la végétation depuis deux millions d'années. Artcom'/Errance, Paris, pp. 179 -217.

Maley, J., 2010. Climate and palaeoenvironment evolution in north tropical Africa from the end of the Tertiary to the Upper Quaternary. Palaeoecology of Africa 30, 227-278.

Maslin, M.A., Shultz, S., Trauth, M.H., 2015. A synthesis of the theories and concepts of early human evolution. Philosophical Transactions of the Royal Society B 370, 1-12.

Ménabréaz, L., Thouveny, N., Bourlès, D.L., Deschamps, P., Hamelin, B., Demory, F., 2011. The Laschamp geomagnetic dipole low expressed as a cosmogenic ^{10}Be atmospheric overproduction at ~41 ka. Earth and Planetary Science Letters 312, 305-317.

Mercader, J., Bennett, T., Esselmont, C., Simpson, S., Walde, D., 2009. Phytoliths in woody plants from the Miombo woodlands of Mozambique. Annals of Botany 104, 91-113.

Morley, R.J., Richards, K., 1993. Gramineae cuticle: a key indicator of Late Cenozoic climatic change in the Niger Delta. Review of Palaeobotany and Palynology 77, 119-127.

Moussa, A., 2010. Les séries sédimentaires fluviatiles, lacustres et éoliennes du bassin du Tchad depuis le Miocène terminal, Ph-D thesis. Université de Strasbourg.

Neumann, K., Fahmy, A., Lespez, L., Ballouche, A., Huysecom, E., 2009. The early holocene palaeoenvironment of Ounjougou (Mali): Phytoliths in a multiproxy context. Palaeogeography, Palaeoclimatology, Palaeoecology 276, 87-106.

New, M., Lister, D., Hulme, M., Makin, I., 2002. A high-resolution data set of surface climate over global land areas. Climate research 21 1-25.

Nishiizumi, K., Imamura, M., Caffe, M.W., Southon, J.R., Finkel, R.C., J., M., 2007. Absolute calibration of ^{10}Be AMS standards. Nuclear Instruments and Methods in Physics Research B 58, 403-413.

Novello, A., 2012. Les phytolithes, marqueurs des environnements mio-pliocènes du Tchad, PhD Thesis. Université de Poitiers.

Novello, A., Barboni, D., Berti-Equille, L., Mazur, J.-C., Poilecot, P., Vignaud, P., 2012. Phytolith signal of aquatic plants and soils in Chad, Central Africa. Review of Palaeobotany and Palynology 178, 43-58.

Olivry, J.-C., Chouret, A., Vuitlaume, G., Lemoalle, J., Bricquet, J.-P., 1996. Hydrologie du lac Tchad. Institut Français de Recherche Scientifique pour le Développement en Coopération, Paris.

Otero, O., Lécuyer, C., Fourel, F., Martineau, F., Mackaye, H.T., Vignaud, P., Brunet, M., 2011. Freshwater fish $\delta^{18}O$ indicates a Messinian change of the precipitation regime in Central Africa. Geology 39, 435-438.

Otero, O., Pinton, A., Mackaye, H.T., Likius, A., Vignaud, P., Brunet, M., 2010. The fish assemblage associated with the Late Miocene Chadian hominid (site TM266, Toros-Menalla, Western Djurab), and its palaeoenvironmental signification. Palaeontographica Acta 292, 21-51.

Pagani, M., Freeman, K.H., Arthur, M.A., 1999. Late Miocene atmospheric CO_2 concentrations and the expansion of C_4 grasses. Science 285, 876-879.

Pagani, M., Liu, Z., LaRiviere, J., Ravelo, A.C., 2010. High Earth-system climate sensitivity determined from Pliocene carbon dioxide concentrations. Nature Geoscience 3, 27-30.

Pound, M.J., Haywood, A.M., Salzmann, U., Riding, J.B., 2012. Global vegetation dynamics and latitudinal temperature gradients during the Mid to Late Miocene (15.97–5.33 Ma). Earth-Science Reviews 112, 1-22.

Prasad, V., Strömberg, C.A.E., Leaché, A.D., Samant, B., Patnaik, R., Tang, L., Mohabey, D.M., Ge, S., Sahni, A., 2011. Late Cretaceous origin of the rice tribe provides evidence for early diversification in Poaceae. Nature Communications 2, 480.

Ravelo, A.C., Andreasen, D.H., Lyle, M., Lyle, A.O., Wara, M.W., 2004. Regional climate shifts caused by gradual global cooling in the Pliocene epoch. Nature 429, 263-267.

Rirongarti, R., 2014. Etude de la variabilité spatiale et temporelle des diatomées actuelles du lac Tchad, Master Thesis. Université de N'Gaoundéré.

Rognon, P., 1967. Climatic influences on the African Hoggar during the Quaternary, based on geomorphologic observations. Annals of the Association of American Geographers 57, 115-127.

Rossouw, L., 2009. The application of fossil grass-phytolith analysis in the reconstruction of late Cenozoic environments in the South African interior, PhD Thesis. University of the Free State, Bloemfontein.

Rossouw, L., Scott, L., 2011. Phytoliths and Pollen, the Microscopic Plant Remains in Pliocene Volcanic Sediments Around Laetoli, Tanzania, in: Harrison, T. (Ed.), Paleontology and Geology of Laetoli: Human Evolution in Context. Springer, New York, pp. 201 - 215.

Round, F.E., Crawford, R.M., Mann, D.G., 1990. The Diatoms, Biology & Morphology of the genera. Cambridge University Press.

Runge, F., 1999. The opal phytolith inventory of soils in central Africa - quantities, shapes, classification, and spectra. Review of Palaeobotany and Palynology 107, 23-53.

Sage, R.F., 2004. The evolution of C_4 photosynthesis. New Phytologist 161, 341-370.

Salzmann, U., Haywood, A.M., Lunt, D.J., Valdes, P.J., Hill, D.J., 2008. A new global biome reconstruction and data-model comparison for the Middle Pliocene. Global Ecology & Biogeography 17, 432-447.

Salzmann, U., Williams, M., Haywood, A.M., Johnson, A.L.A., Kender, S., Zalasiewicz, J., 2011. Climate and environment of a Pliocene warm world. Palaeogeography, Palaeoclimatology, Palaeoecology 309, 1-8.

Sangster, A.G., Parry, D.W., 1969. Some factors in relation to bulliforrn cell silicification in the grass Leaf. Annals of Botany 33, 315-323.

Schneider, J.-L., 1989. Géologie et hydrogéologie de la République du Tchad, PhD Thesis. Université des Sciences, Avignon.

Schuster, M., Duringer, P., Ghienne, J.-F., Roquin, C., Sepulchre, P., Moussa, A., Lebatard, A., Mackaye, H.T., Likius, A., Vignaud, P., Brunet, M., 2009. Chad Basin: Paleoenvironments of the Sahara since the Late Miocene. Comptes Rendus Geoscience 341, 603-611.

Schuster, M., Duringer, P., Ghienne, J.-F., Vignaud, P., Mackaye, H.T., Likius, A., Brunet, M., 2006. The Age of the Sahara Desert. Science 311, 821-821.

Schuster, M., Duringer, P., Nel, A., Brunet, M., Vignaud, P., Mackaye, H.T., 2000.

Découverte de termitières fossiles dans les sites à Vertébrés du Pliocène tchadien : description, identification et implications paléoécologiques. Compte Rendus de l'Académie des Sciences de Paris 331, 15-20.

Schuster, M., Roquin, C., Duringer, P., Brunet, M., Fontugne, M., Mackaye, H.T., Vignaud, P., Ghienne, J.-F., 2005. Highlighting Holocene Lake Mega-Chad palaeoshorelines from space. Quaternary Science Reviews 24, 1821-1827.

Senut, B., Pickford, M., Gommery, D., Mein, P., Cheboi, K., Coppens, Y., 2001. First hominid from the Miocene (Lukeino Formation, Kenya). Comptes Rendus de l'Académie des Sciences de Paris 332, 137-144.

Servant-Vildary, S., 1978. Etude des diatomées et paléolimnologie du Bassin tchadien au Cénozoïque supérieur, Travaux et Documents de l'ORSTOM, 82, 2 tomes, Paris, p. 346.

Servant, M., 1973. Séquences continentales et variations climatiques : Evolution du bassin du Tchad au Cénozoïque supérieur. ORTSOM, Paris, p. 159.

Strömberg, C.A.E., 2003. The origin and spread of grass-dominated ecosystems during the Tertiary of North America and how it relates to the evolution of hypsodonty in equids, PhD Thesis. University of California, Berkeley.

Strömberg, C.A.E., 2009. Methodological concerns for analysis of phytolith assemblages: Does count size matter? Quaternary International 193, 124-140.

Strömberg, C.A.E., 2011. Evolution of grasses and grassland ecosystems. Annual Review of Earth Planetary Sciences 39, 517-544.

Tipple, B.J., Pagani, M., 2010. A 35 Myr North American leaf-wax compound-specific carbon and hydrogen isotope record: implications for C_4 grasslands and hydrologic cycle dynamics. Earth and Planetary Science Letters 299, 250-262.

Vignaud, P., Duringer, P., Mackaye, H.T., Likius, A., Blondel, C., Boisserie, J.-R., Bonis, L.d., Eisenmann, V., Etienne, M.-E., Geraads, D., Guy, F., Lehmann, T., Lihoreau, F., Lopez-Martinez, N., Mourer-Chauviré, C., Otero, O., Rage, J.-C., Schuster, M., Viriot, L., Zazzo, A., Brunet, M., 2002. Geology and Palaeontology of the Upper Miocene Toros-Menalla hominid locality, Djurab Desert, Northern Chad. Nature 418, 152-155.

Vincens, A., Buchet, G., Servant, M., collaborators, E.M., 2010. Vegetation response to the "African Humid Period" termination in Central Cameroon (7°N) - new pollen insight from Lake Mbalang. Climate of the Past 6, 281-294.

Wheeler, P.E., 1991a. The influence of bipedalism on the energy and water budgets of early hominids Journal of Human Evolution 21, 117-136.

Wheeler, P.E., 1991b. The thermoregulatory advantages of hominid bipedalism in open equatorial environments: the contribution of increased convective heat loss and cutaneous evaporative cooling Joumal of fHuman Evolution 21, 107-115.

White, T.D., 1985. The hominids ofHadar and Laetoli: an element-by-element comparison of the dental samples, in: Delson, E. (Ed.), Ancestors: the Hard Evidence. A. R. Liss, New York, pp. 219-240.

White, T.D., Suwa, G., Asfaw, B., 1994. *Australopithecus ramidus*, a new species of hominid from Aramis, Ethiopia. Nature 371, 306-312.

WoldeGabriel, G., Ambrose, S.H., Barboni, D., Bonnefille, R., Bremond, L., Currie, B., DeGusta, D., Hart, W.K., Murray, A.M., Renne, P.R., Jolly-Saad, M.C., Stewart, K.M., White, T.D., 2009. The geological, isotopic, botanical, invertebrate, and lower vertebrate surroundings of *Ardipithecus ramidus*. Science 326, 65e61-65.

Zazzo, A., Bocherens, H., Brunet, M., Beauvilain, A., Billiou, D., Mackaye, H.T., Vignaud, P., Mariotti, A., 2000. Herbivore paleodiet and paleoenvironmental changes in Chad during the Pliocene using stable isotope ratios of tooth enamel carbonate. Paleobiology 26, 294-309.

Accepted manuscript now published in *Palaeogeography, Palaeoclimatology, Palaeoecology* (2015) 430: 85 - 103 〈10.1016/j.palaeo.2015.04.013〉

Figures and Tables

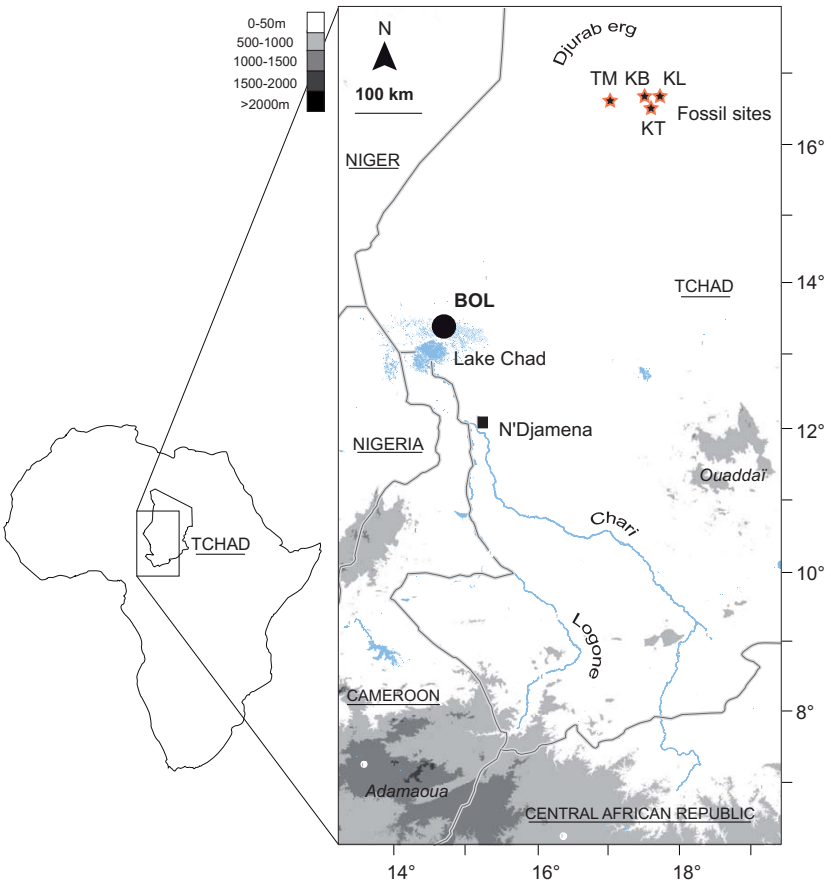

Fig.1 Map locating the Bol borehole in the Lake Chad archipelago, about 400 km to the south of the Mio-Pliocene fossil sites of the Djurab desert (stars). TM: 7.3±0.1 Ma (type-locality of *Sahelanthropus tchadensis*), KB: 5.4±0.6 Ma, KL: 4.0±0.1 Ma, and KT: 3.6±0.1 Ma (type-locality of *Australopithecus bahrelghazali*) (Lebatard et al., 2010).

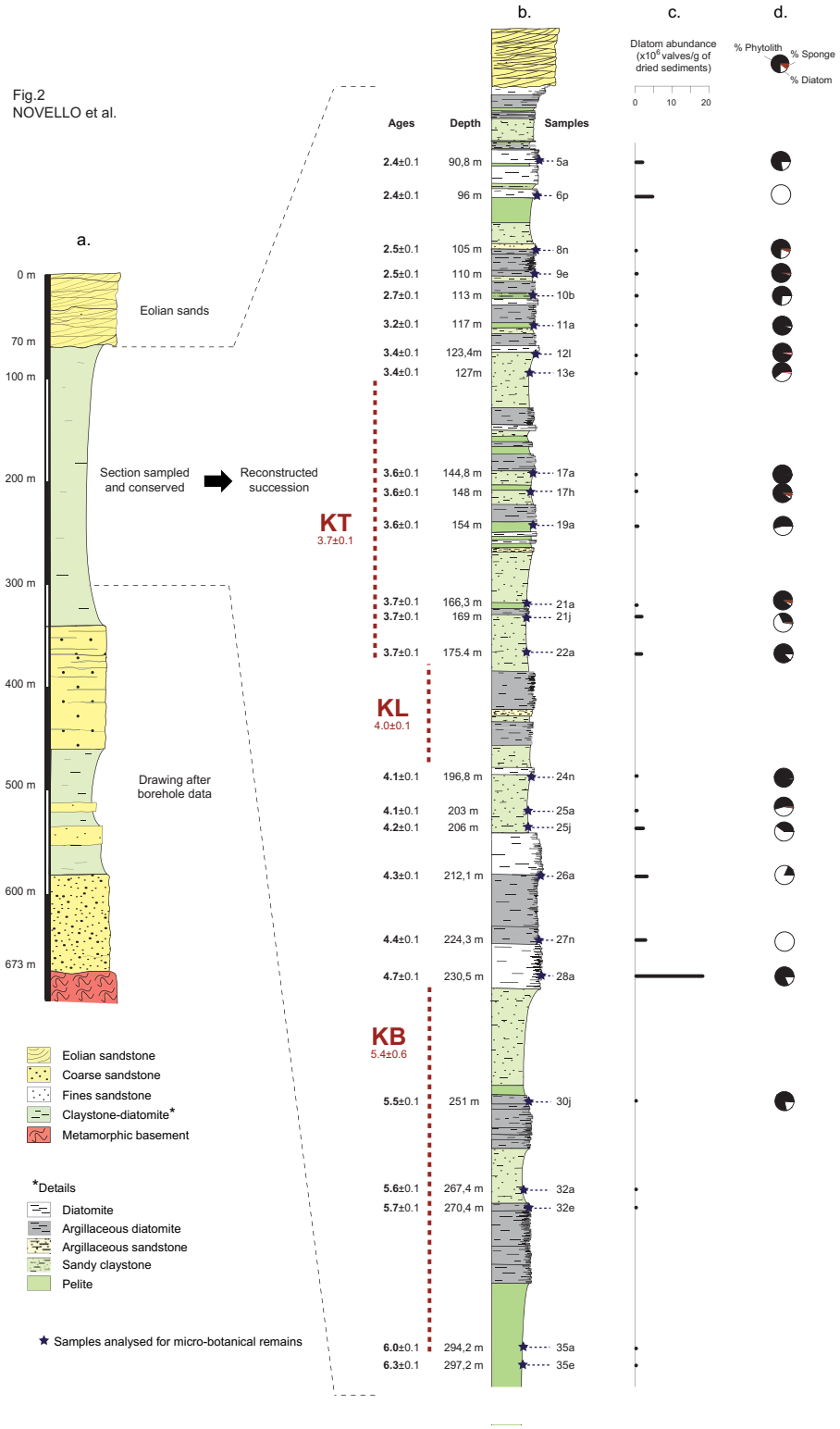

Fig.2 Sedimentology of Bol borehole and stratigraphical positioning of the 25 studied samples (**a**. general synthesis; **b**. detailed sequence reconstructed from preserved cuttings), **c.** diatom concentration in the samples (number of valves/g of dry sediments), and **d.** quantification of phytoliths, diatoms, and sponge spicules recovered in the silicified assemblages. The time range of the Mio-Pliocene fossil sites from the Djurab is given in parallel to the chronology of Bol borehole.

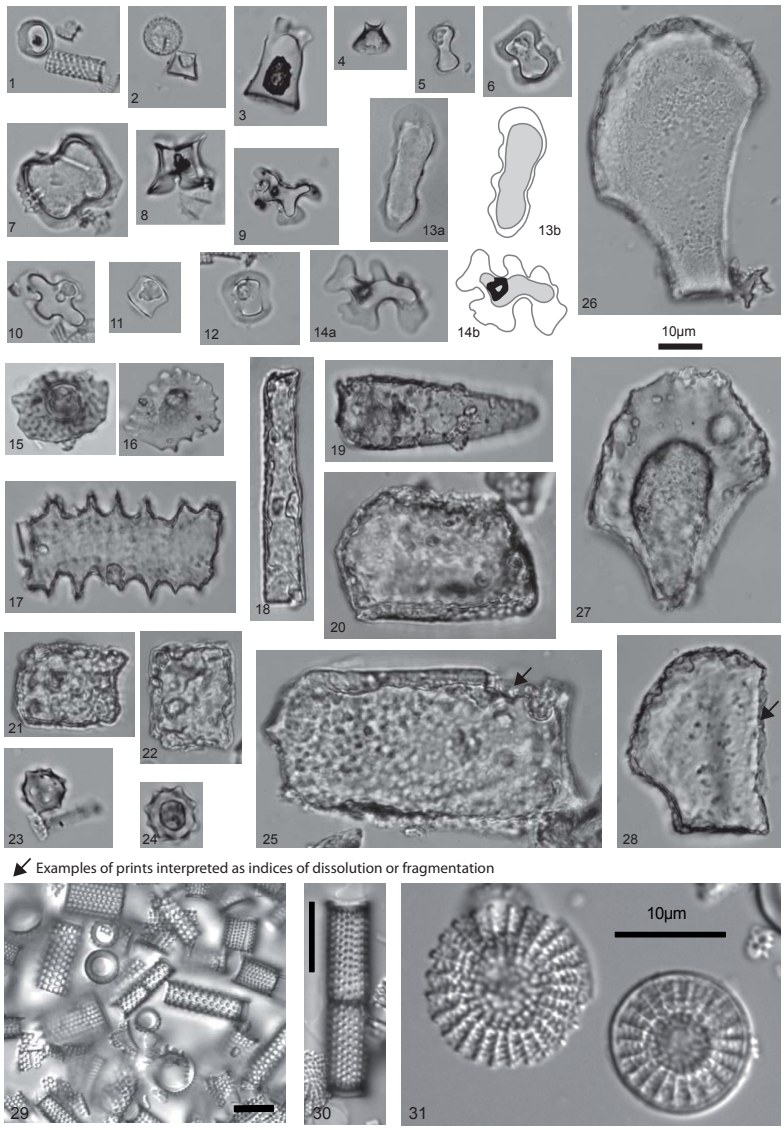

Fig.3 Selected phytolith types and diatom species observed in the fossil sediments of Bol. Phytolith IDs follow the classification of Novello et al. (2012). 1-2. Rondel, conical, top truncated: Ro1 (1: in top view, 2: in side view) (near diatoms); 3. Rondel, conical, top truncated, tall (h>15µm): Ro7; 4. Rondel, conical, top keeled: Ro2; 5. Bilobate, short and tabular, round lobes: Bi2; 6. Bilobate, short and trapeziform, length>height: Bi11; 7. Bilobate, short and tabular, missing shank: Bi9; 8. Bilobate, short and trapeziform, length=height: Bi12; 9. Bilobate, trapeziform, concave lobes: Bi14; 10. Cross, trapeziform, 4-lobed, cross top: Cr5; 11. Saddle, tabular long: S3; 12. Saddle, trapeziform, base round and vaguely constricted: S4; 13a-b. Polylobate, trapeziform, base regularly sinuate: Poly4*; 14a-b. Polylobate, trapeziform, base irregularly sinuate with closed concavities/convexities: Poly3*; 15. Plate, regularly scorbiculate with a short depressed cone in the center: Pla4; 16. Plate, sinuous shape, knobby apex: Pla5; 17. Elongate, tabular, echinate margins: El3; 18. Elongate, tabular, smooth margins: El3; 19. Acicular, psilate, pitting of dissolution/altered: Aci1; 20-22, 25. Blocky, cubic to parallelepipedal, prints of dissolution/altered on surface: Blo3,-6 or -7; 23-24. Globular, echinate: Glo1; 26-28. Blocky, cuneiform with prints of dissolution/altered on surface (28: broken cuneiform): Blo4; 29. Diatomite dominated by *Aulacoseira granulata*, sample 10b; 30. *Aulacoseira granulata*; 31. *Stephanodiscus carconensis* (var. *pusilla*). *New types

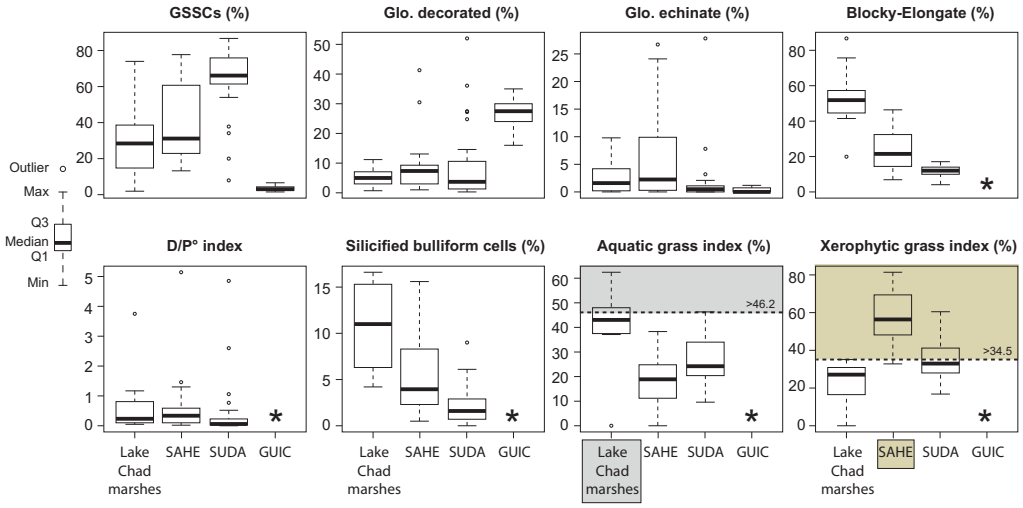

Fig.4 Box-plots showing the abundance patterns of the main phytolith indicators and indices considered in this study according to modern sub-Saharan environments: Lake Chad marshes, Sahelian, and Sudanian vegetation, and Guineo-Congolian vegetations (from Runge, 1999). Grey areas indicate the range of Aquatic (Iaq) and Xerophytic (Ixe) grass indices characterizing a phytolith signal from present-day Lake Chad marshy grasses and from Sahelian grasses.

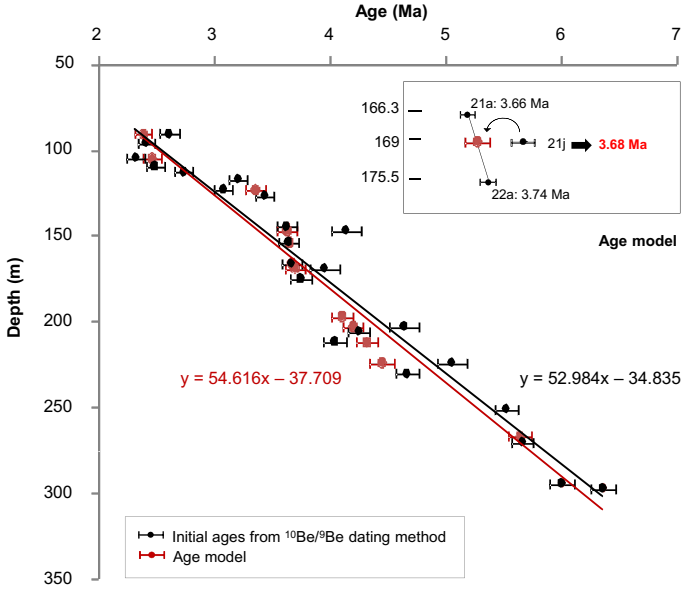

Fig.5 Age model estimated from the $^{10}Be/^{9}Be$ initial age values. Calculation method for modeling ages is illustrated for sample 21j as an example.

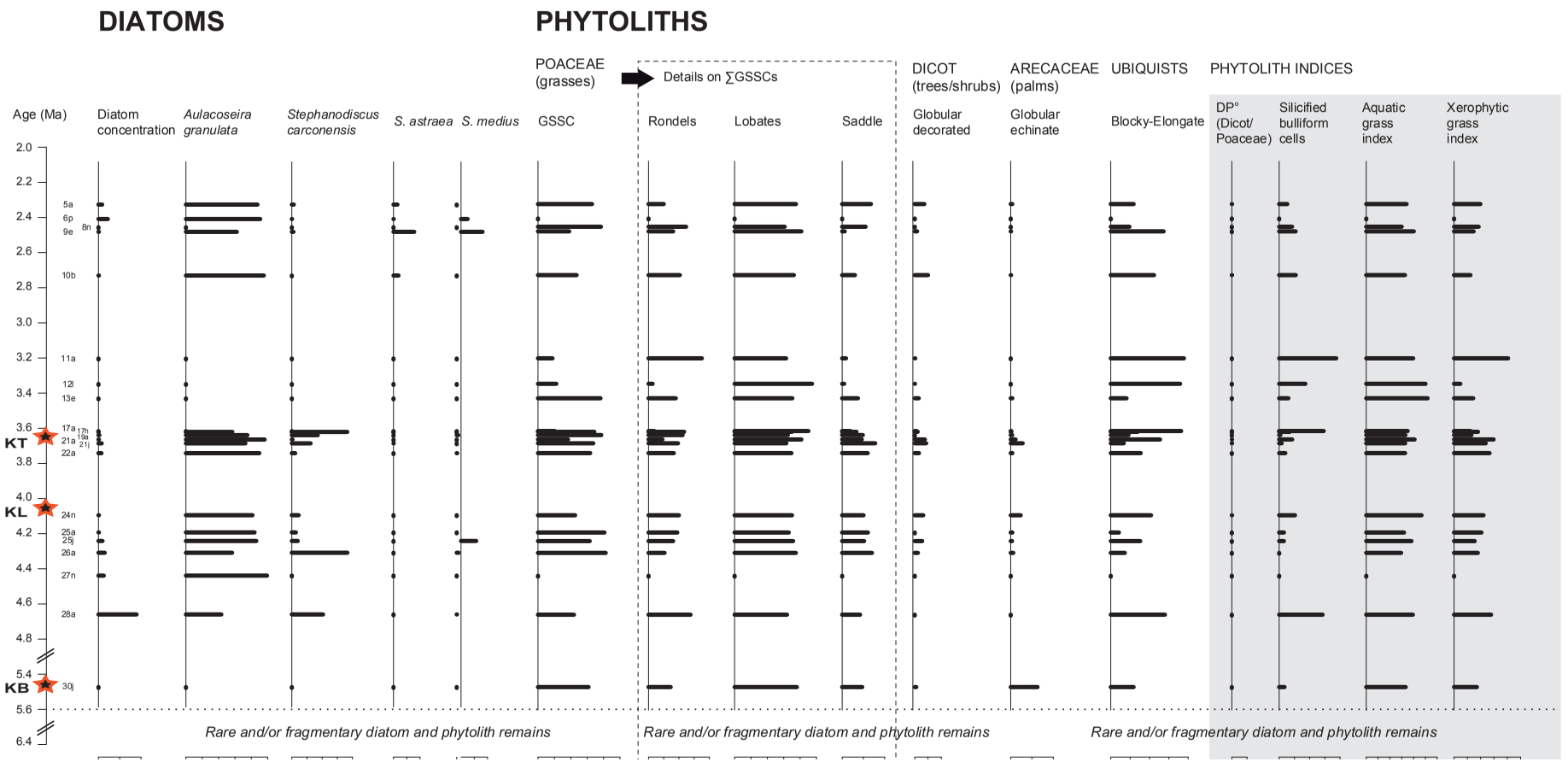

Fig.6 Abundance diagrams of main diatom species, and phytolith types and indices (in grey) observed in the fossil assemblages of Bol. A quantitative estimation of the abundance of diatoms in the sediments is also provided. Stars indicate fossil localities of the Djurab (northern Chad) on the time scale: KB (5.4±0.6 Ma), KL (4.0±0.1 Ma), and KT (3.6±0.1 Ma).

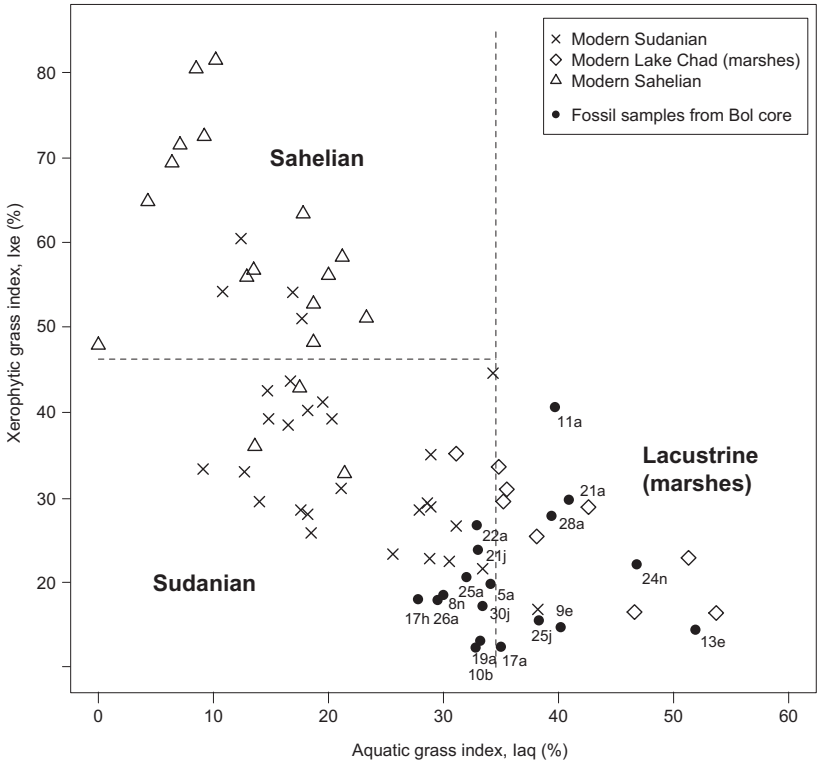

Fig.7 Plot comparing the distribution of the 25 fossil samples with modern samples from Chad according to the Iaq and Ixe grass phytolith indices. Threshold values (dotted lines) were estimated using the rpart function (R.13.0), as also indicated on modern box-plots (Fig.4).

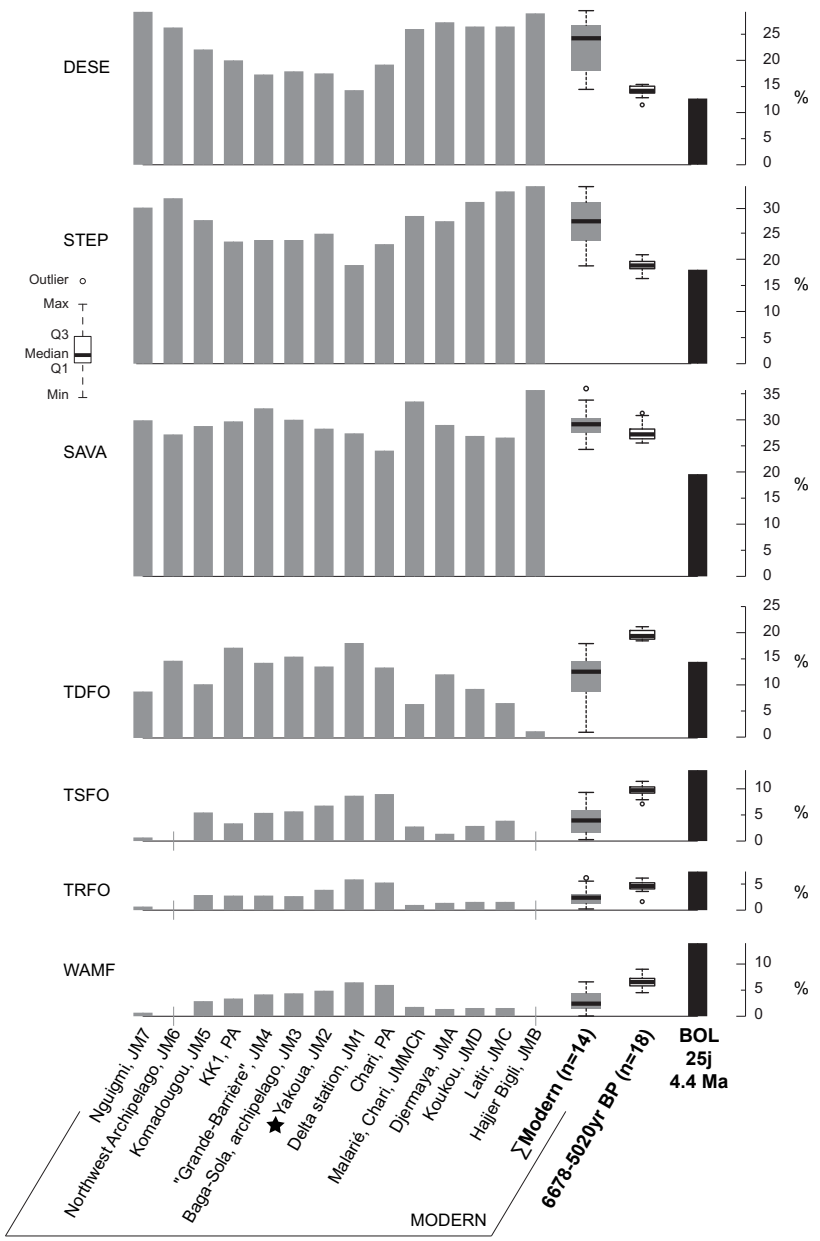

Fig.8 Biome scores inferred from the fossil pollen data of Bol sample 25j (dated 4.2 Ma) compared to biome scores calculated for modern (Maley, 1972, 1981; Amaral et al.. 2013) and Holocene (6678-5020 yr BP) data (Amaral et al., 2013) from Lake Chad. Biome classification follows Lézine et al. (2009): DESE: desert; STEP: steppe; SAVA: savanna; TDFO: tropical dry forest; TSFO: tropical seasonal forest; TRFO: tropical rain forest; WAMF: warm mixed-forest.

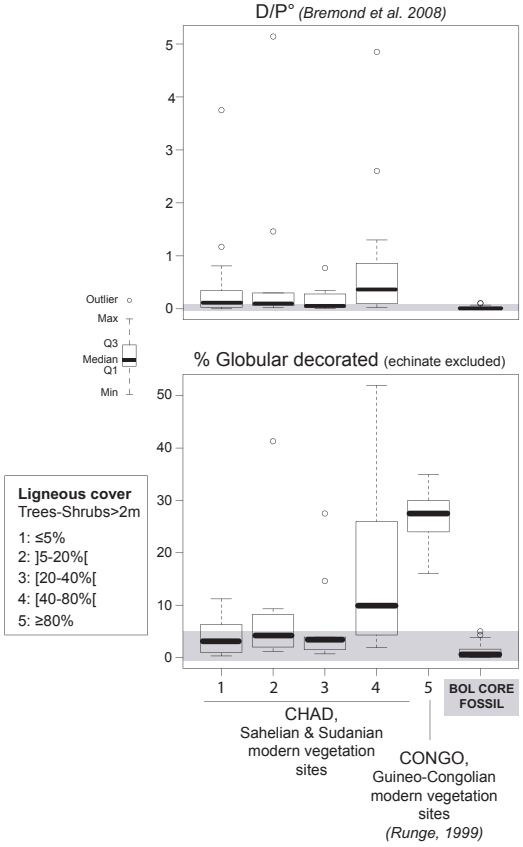

Fig.9 Box-plots of the values of D/P° phytolith index values and of the percentages of globular decorated phytoliths (echinate excluded) in the Bol fossil assemblages, and compared with those observed from non-forested soils of Chad, and from tropical evergreen forest soils of the Democratic Republic of Congo, DRC (Runge, 1999). Modern environments are classified according to their percentages of ligneous cover directly estimated in the field for Chadian environments, and estimated by satellite for forested environments from DRC (see Barboni et al. 2007). Grey areas draw the ranges of D/P° values and of the globular decorated phytolith percentages obtained for the fossil samples of Bol.

Accepted manuscript now published in *Palaeogeography, Palaeoclimatology, Palaeoecology* (2015) 430: 85 - 103 〈10.1016/j.palaeo.2015.04.013〉

Samples	Depth (m)	^{10}Be (.10^{7} at.g^{-1})		^{9}Be (.10^{15} at.g^{-1})		^{10}Be/^{9}Be (.10^{-9})		Age (Ma)		Age model (Ma)	
BOL 74[§]	74.0	13.044	± 0.449	5.163	± 0.061	25.263	± 0.919	-			
BOL 5a	90.8	3.399	± 0.065	4.911	± 0.030	6.920	± 0.139	2.61	± 0.08	**2.38**	± **0.07**
BOL6p	96.0	7.660	± 0.073	10.028	± 0.042	7.639	± 0.080	2.41	± 0.07	**2.41**	± **0.07**
BOL 8n	105.0	4.136	± 0.064	5.174	± 0.053	7.994	± 0.149	2.32	± 0.08	**2.45**	± **0.08**
BOL 9c	110.0	5.298	± 0.075	7.192	± 0.053	7.366	± 0.117	2.48	± 0.08	**2.48**	± **0.08**
BOL 10b	113.0	6.449	± 0.082	9.916	± 0.115	6.504	± 0.112	2.73	± 0.08	**2.73**	± **0.08**
BOL 11a	117.0	6.177	± 0.093	12.034	± 0.089	5.134	± 0.086	3.20	± 0.08	**3.20**	± **0.08**
BOL 12l	123.4	6.221	± 0.067	11.375	± 0.089	5.469	± 0.073	3.08	± 0.08	**3.35**	± **0.08**
BOL 13e	127.0	2.851	± 0.050	6.219	± 0.021	4.584	± 0.082	3.43	± 0.08	**3.43**	± **0.08**
BOL 17a	144.8	3.345	± 0.052	8.006	± 0.066	4.178	± 0.074	3.62	± 0.08	**3.62**	± **0.08**
BOL 17h[§]	147.0	2.001	± 0.098	6.202	± 0.066	3.226	± 0.161	4.13	± 0.13	**3.62**	± **0.08**
BOL 19a	154.0	2.758	± 0.049	6.678	± 0.059	4.129	± 0.082	3.64	± 0.09	**3.64**	± **0.09**
BOL 21a	166.3	3.277	± 0.057	8.036	± 0.052	4.078	± 0.076	3.66	± 0.08	**3.66**	± **0.08**
BOL 21j[§]	169.3	2.481	± 0.119	7.013	± 0.021	3.538	± 0.170	3.95	± 0.12	**3.69**	± **0.09**
BOL 22a	175.5	2.494	± 0.053	6.359	± 0.036	3.922	± 0.086	3.74	± 0.09	**3.74**	± **0.09**
BOL 24n	197.0	-	- -	-	- -	-	- -	-	- -	**4.09**	± **0.09**
BOL 25a[§]	203.0	1.595	± 0.082	6.362	± 0.035	2.507	± 0.129	4.64	± 0.13	**4.19**	± **0.09**
BOL 25j	206.0	2.391	± 0.049	7.828	± 0.087	3.054	± 0.071	4.24	± 0.09	**4.24**	± **0.09**
BOL 26a	212.1	2.193	± 0.068	6.479	± 0.052	3.385	± 0.109	4.04	± 0.10	**4.31**	± **0.09**
BOL 27n[§]	224.3	1.829	± 0.087	8.943	± 0.042	2.045	± 0.097	5.04	± 0.13	**4.44**	± **0.10**
BOL 28a	230.5	1.531	± 0.045	6.175	± 0.079	2.479	± 0.080	4.66	± 0.10	**4.66**	± **0.10**
BOL 30j	251.0	1.432	± 0.040	8.866	± 0.026	1.615	± 0.045	5.52	± 0.10	**5.52**	± **0.10**
BOL 32a[§]	269.0	1.803	± 0.095	17.644	± 0.114	1.022	± 0.054	6.43	± 0.14	**5.63**	± **0.10**
BOL 32e	270.4	2.172	± 0.047	14.430	± 0.027	1.506	± 0.033	5.66	± 0.10	**5.66**	± **0.10**
BOL 35a	294.2	0.664	± 0.019	5.218	± 0.028	1.273	± 0.037	5.99	± 0.10	**5.99**	± **0.10**
BOL 35e	297.2	1.379	± 0.044	12.946	± 0.030	1.065	± 0.034	6.35	± 0.11	**6.35**	± **0.11**

Table 1 Authigenic Be concentrations, ^{10}Be/^{9}Be ratios, and ages (initial ages and age model) for the 25 Bol samples. Initial ages re-estimated from age model are boxed. [§]Samples specifically measured at the AMS Tandetron facility (Gif/Yvette, France).

Table 2. Novello et al.

			PHY/DIA/SPO			DIATOMS							PHYTOLITHS and INDICES																							
Sample	Depth (m)	Age (Ma)	Phytoliths	Diatoms	Sponge spicules	Diatom concentration (*10⁶ number of valves/g of dry sediments)	Diatom diversity (number of species)	*Aulacoseira granulata* (Ehrenberg) Simonsen	*Stephanodiscus carconensis* Grunow and varieties	Other species*	*including epiphytic species	∑ GSSC*	*including Rondel	*including Bilobate	*including Cross	*including Polylobate trapeziform	*including Saddle	∑ Blocky*	*including Silicified bulliform cells (Fs index)	∑ Elongate	∑ Globular*	*including Globular decorated (other than echinate)	*including Globular echinate	∑ Acicular	∑ Epidermal silicified structure	∑ Polyhedral body	∑ Polyhedral plate*	* including Cyperaceae-papillae	∑ Unclassified	(Iaq) Aquatic grass index	(Ixe) Xerophytic grass index	D/P° (tree-cover index)					
BOL 5a	90.8	**2.4 ± 0.1**	77.7	21.8	0.5	*1.7*	14	89.0	1.3	8.2	0.0	66.0	10.0	55.9	19.0	1.5	13.5	10.2	5.3	13.2	6.6	3.6	0.7	3.6	0.0	0.0	1.0	0.3	0.0	34.1	19.8	*0.06*			
BOL 6p	96.0	**2.4 ± 0.1**	0.0	100.0	0.0	*4.4*	16	92.2	0.2	5.0	0.7	-	-	-	-	-	-	-	-	-	-	-	-	-	-	-	-	-	-	-	-	-			
BOL 8n	105.0	**2.5 ± 0.1**	74.4	20.1	5.5	-	-	-	-	-	-	76.8	24.7	41.9	19.2	3.2	11.0	17.6	8.4	1.8	0.0	0.0	0.0	2.5	0.4	1.0	1.0	0.0	0.4	30.0	18.5	*0.00*			
BOL 9e	110.0	**2.5 ± 0.1**	95.0	2.9	2.1	*0.2*	15	65.6	1.1	14.1	1.1	38.1	16.2	57.8	23.7	1.2	1.2	28.9	10.8	25.8	3.5	0.9	0.2	3.5	0.0	0.0	1.0	0.2	0.0	40.2	14.7	*0.02*			
BOL 10b	113.0	**2.7 ± 0.1**	73.8	26.2	0.0	*0.2*	6	95.7	0.0	2.4	0.0	47.1	20.6	48.4	24.1	1.0	6.0	27.2	10.9	17.5	6.1	5.0	0.2	0.5	0.0	0.0	7.0	0.0	0.0	32.8	12.3	*0.11*			
BOL 11a	117.0	**3.2 ± 0.1**	94.5	5.3	0.1	-	-	-	-	-	-	17.7	35.1	40.1	22.7	0.4	1.8	54.9	37.5	20.6	0.2	0.2	0.0	6.3	0.1	0.0	2.0	0.1	0.1	39.7	40.6	*0.01*			
BOL 12l	123.4	**3.3 ± 0.1**	96.1	0.3	3.6	-	-	-	-	-	-	22.3	2.7	60.6	34.0	1.8	0.9	42.8	17.2	28.8	0.1	0.1	0.0	5.9	0.0	0.0	1.0	0.1	0.0	50.1	4.7	*0.00*			
BOL 13e	127.0	**3.4 ± 0.1**	61.0	37.1	1.8	-	-	-	-	-	-	76.2	17.9	33.7	36.7	4.2	7.4	12.1	6.0	4.2	2.3	1.5	0.8	2.3	0.8	0.0	3.0	0.0	1.1	51.9	14.4	*0.02*			
BOL 17a	144.8	**3.6 ± 0.1**	98.2	0.3	1.5	-	-	-	-	-	-	20.3	3.8	46.0	44.0	2.4	3.8	54.9	29.2	17.8	1.1	0.7	0.3	5.7	0.0	0.0	3.0	0.1	0.0	35.0	12.4	*0.03*			
BOL 17h	147.0	**3.6 ± 0.1**	89.2	4.9	5.9	*0.1*	9	57.5	36.5	1.8	1.0	68.7	23.4	43.6	26.3	0.0	6.7	15.5	6.9	12.3	1.4	1.1	0.3	1.7	0.0	0.0	0.0	0.0	0.3	27.8	18.0	*0.02*			
BOL 19a	154.0	**3.6 ± 0.1**	54.2	45.4	0.4	*0.4*	13	76.1	17.1	6.2	2.7	77.2	22.4	34.9	30.0	3.0	9.7	4.6	0.7	13.7	1.0	0.0	0.0	2.6	0.0	0.0	3.0	0.3	0.0	33.2	13.1	*0.00*			
BOL 21a	166.3	**3.7 ± 0.1**	89.9	4.9	5.2	*0.2*	8	96.3	0.5	3.2	0.8	36.7	9.2	48.3	33.2	0.0	9.2	30.2	8.5	20.7	6.0	3.8	2.3	5.8	0.0	0.0	3.0	0.6	0.0	40.9	29.7	*0.10*			
BOL 21j	169.0	**3.7 ± 0.1**	32.1	65.6	2.3	*1.5*	16	73.2	12.4	10.0	0.5	67.5	19.4	41.5	21.6	1.9	15.5	6.6	1.6	7.5	9.8	4.3	5.6	3.0	1.0	0.0	5.0	1.3	3.0	33.0	23.8	*0.06*			
BOL 22a	175.5	**3.7 ± 0.1**	87.1	12.4	0.5	*1.4*	9	93.8	2.2	3.7	1.0	63.6	16.6	48.0	21.3	2.1	12.0	12.6	4.0	18.2	2.9	1.6	0.8	2.6	0.0	0.0	0.0	0.0	0.0	32.9	26.7	*0.02*			
BOL 24n	197.0	**4.1 ± 0.1**	96.1	2.9	1.0	*0.2*	10	85.0	4.5	10.5	2.4	45.2	20.0	47.7	22.3	0.0	10.0	21.3	10.3	20.2	8.6	3.2	4.7	3.4	0.0	0.0	6.0	1.3	0.0	46.8	22.1	*0.07*			
BOL 25a	203.0	**4.2 ± 0.1**	54.3	43.5	2.1	*0.2*	13	86.1	2.7	3.2	0.2	81.1	18.9	41.9	24.2	2.9	12.1	4.3	3.1	3.9	0.8	0.0	0.8	4.7	0.4	0.0	1.0	0.0	4.3	32.0	20.6	*0.00*			
BOL 25j	206.0	**4.2 ± 0.1**	40.0	59.9	0.1	*1.9*	12	88.9	3.9	1.5	0.1	63.1	16.2	43.0	28.5	2.0	10.3	3.4	3.1	27.0	4.7	2.8	0.6	0.9	0.0	0.0	3.0	0.0	0.0	38.3	15.5	*0.04*			
BOL 26a	212.1	**4.3 ± 0.1**	18.2	81.8	0.0	*2.9*	7	61.5	36.6	1.2	0.0	82.6	10.5	43.2	31.6	0.7	14.0	1.7	0.0	12.8	2.3	1.2	1.2	0.6	0.0	0.0	0.0	0.0	0.0	29.5	17.9	*0.01*			
BOL 27n	224.0	**4.4 ± 0.1**	0.0	100.0	0.0	*2.5*	2	99.2	0.0	0.8	0.0	-	-	-	-	-	-	-	-	-	-	-	-	-	-	-	-	-	-	-	-	-			
BOL 28a	230.5	**4.7 ± 0.1**	81.6	18.2	0.2	*17.9*	23	49.7	20.6	29.5	4.0	43.8	27.6	40.9	23.2	0.0	8.4	51.4	28.5	4.8	0.0	0.0	0.0	0.0	0.0	0.0	0.0	0.0	0.0	39.4	27.8	*0.00*			
BOL 30j	251.0	**5.5 ± 0.1**	78.3	20.4	1.3	-	-	-	-	-	-	61.7	14.6	55.1	20.9	0.0	9.4	6.4	3.5	17.1	13.5	0.6	12.6	1.3	0.0	0.0	0.0	0.0	0.0	33.4	17.2	*0.01*			
BOL 32a	267.0	**5.6 ± 0.1**	-	-	-	-	-	-	-	-	-	-	-	-	-	-	-	-	-	-	-	-	-	-	-	-	-	-	-	-	-	-			
BOL 32e	270.4	**5.7 ± 0.1**	-	-	-	-	-	-	-	-	-	-	-	-	-	-	-	-	-	-	-	-	-	-	-	-	-	-	-	-	-	-			
BOL 35a	294.2	**6.0 ± 0.1**	-	-	-	-	-	-	-	-	-	-	-	-	-	-	-	-	-	-	-	-	-	-	-	-	-	-	-	-	-	-			
BOL 35e	297.2	**6.4 ± 0.1**	-	-	-	-	-	-	-	-	-	-	-	-	-	-	-	-	-	-	-	-	-	-	-	-	-	-	-	-	-	-			

Table 2 Synthesis of the diatom and phytolith data for the 25 Bol samples. The table also includes the estimated relative abundance of phytolith (PHY), diatom (DIA), and sponge spicules (SPO) particles in the silicified particle assemblages. Phytolith and diatom data are expressed in %, except diatom concentration and D/P° ratio). The total sum of underlined phytolith categories gives 100%. The $^{10}Be/^{9}Be$ age values indicated are those derived from the age model (see Fig.5).

	Leersia hexandra				***Phragmites australis***	
	Bi2	Bi8	Bi11	Poly1	S4	S5
				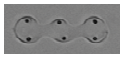		
C_4 grass species (from Novello et al. 2012)						
Aristidoideae						
Aristida stipoides Lam.	x	x	x			
Chloridoideae						
Ctenium elegans Kunth		x				
Cynodon dactylon (L.) Pers.		x				x
Dactyloctenium aegyptium (L.) Willd.						x
Eragrostis pilosa (L.) P. Beauv.		x				x
Eragrostis tremula Steud.						x
Sporobolus cordofanus (Steud.) Coss.					x	x
Panicoideae						
Andropogon gayanus Kunth	x	x				x
Andropogon pseudapricus Stapf	x	x		x		
Brachiaria xantholeuca (Schinz) Stapf		x	x	x		
Cenchrus biflorus Roxb.	x	x				
Diheteropogon amplectens (Nees) Clayton	x	x	x	x		
Echinochloa pyramidalis (Lam.) Hitchc. & Chase	x	x		x		
Hyparrhenia bagirmica (Stapf) Stapf		x	x	x		
Hyparrhenia barteri (Hack.) Stapf		x		x		
Hyparrhenia dissoluta (Nees es Steud.) Clayton		x	x			
Loudetia simplex (Nees) Hubb.		x				
Loudetia togoensis (Pilg.) Hubb.	x	x				
Panicum anabaptistum Steud.	x	x		x		
Panicum fluvicola Steud.	x		x	x		
Panicum laetum Kunth	x	x	x	x		
Panicum subalpinum Kunth	x	x	x			
Panicum turgidum Forssk.		x	x			
Pennisetum pedicellatum Trin.	x	x	x			
Setaria sphacelata (Schumach.) Moss				x		
Vetiveria nigritana (Benth.) Stapf						x
Vossia cuspidata (Roxb.) Grill.		x	x			

Table 3 Occurrences of the bilobate, cross, and tabular polylobate phytolith types produced by the aquatic C_3 grass species *Leersia hexandra* on the one hand, and of the saddle phytolith types produced by the aquatic C_3 grass species *Phragmites australis* on the other hand, in 27 tropical C_4 grass species largely distributed presently in the Lake Chad basin. Original data are from Novello et al. 2012. Scale bar: 10µm.

Supplementary material

Table S1 Detailed diatom and phytolith counts for Bol samples. S: Sterile.

Table S2 Detailed pollen count for Bol sample 25j along with pollen taxa assignment to plant functional types, and biome scores.

Table S1

ID samples, BOL	5a	6p	8n	9e	10b	11a	12l	13e	17a	17h	19a	21a	21j	22a	24n	25a	25j	26a	27n	28a	30j	32a	32e	35a	35e
DIATOMS (by species)																									
Amphora libyca	3	8															5	8		2					
Amphora ovalis													1												
Aulacoseira ambigua	4	32		9	5					3	4			17	9		31	55		47					
Aulacoseira granulata	481	2113		168	884					227	386	605	622	364	201	344	907	607	1229	288					
Aulacoseira granulata angustissima	42																			27					
Aulacoseira italica tenuissima	5																								
Aulacoseira muzzanensis											1					9									
Aulacoseira pyxis													3												
Cocconeis placentula																1									
Coscinodiscus dispar																				90					
Coscinodiscus praelacustris	31																								
Coscinodiscus praelacustris minor	5										8	3		9	13										
Craticula sp.				2																					
Cyclostephanos damasii		8		13																					
Cyclotella meneghiniana				3							2					1				3					
Cyclotella nov. spec.		3																		7					
Cyclotella ocellata															4										
Cyclotella pygmeae	6																								
Cyclotella omarensis													31												
Cyclotella stelligera		6		2	8							8	11	2	1	4	2								
Cymbella minuta													9												
Cymbella aff. *silesiaca*																2									
Cymbella sp.																			10						
Cymbella silesiaca		51			13						2	2					1	5		3					
Cymbella ventricosa	2																								
Eunotia sp.																	1			2					
Fragilaria brevistriata				3											1										
Fragilaria construens		22		10	1							2	2		1		2			20					
Fragilaria crotonensis	2																								
Fragilaria pinnata																1	4			2					
Fragilaria hungarica													20												
Fragilaria fonticola		1																							
Fragilaria ulna																				8					
Gomphonema gracile		17												1						4					
Navicula aff. *cryptotenella*																3									
Navicula confervacea				3						4	14	5	4	3	6					23					
Navicula cryptocephala													7												
Navicula goepertiana				2						3	4									3					
Nitzschia amphibia																				20					

Table S1

ID samples, BOL	5a	6p	8n	9e	10b	11a	12l	13e	17a	17h	19a	21a	21j	22a	24n	25a	25j	26a	27n	28a	30j	32a	32e	35a	35e
Nitzschia compressa																	1								
Nitzschia sp.											1									15					
Nitzschia sp. (2)																				8					
Pinnularia sp.																				3					
Rhopalodia gibba																				2					
Rhopalodia sp.											1														
Stephanodiscus aff. *damasii*				9																					
Stephanodiscus aff. *medius*										17			37			33									
Stephanodiscus astrea	3	2			18								1												
Stephanodiscus astrea carconensis	6			21																					
Stephanodiscus carconensis		4								125			82												
Stephanodiscus carconensis minor																11									
Stephanodiscus carconensis pusilla	8	1		3						21	88	3	24	9	11		41	394		150					
Stephanodiscus medius		59		22							3			1			60	7		1					
Tabelaria flocculosa																1									
Sum total	**598**	**2327**	**S**	**270**	**929**	**S**	**S**	**S**	**S**	**400**	**514**	**628**	**854**	**406**	**247**	**410**	**1055**	**1076**	**1239**	**728**	**S**	**S**	**S**	**S**	**S**

Table S1

ID samples, BOL	5a	6p	8n	9e	10b	11a	12l	13e	17a	17h	19a	21a	21j	22a	24n	25a	25j	26a	27n	28a	30j	32a	32e	35a	35e
PHYTOLITHS (by types)																									
Grass Silica Short Cells (GSSCs)																									
Rondels																									
Ro1	10		20	13	10	88	1	13	2	7	14	6	9	10	13	11	16	4		25	9				
Ro2			11	1			2	8	1	7	20	1	13	11	6	2	7	3		10	3				
Ro3			1	1				3		33	4	1	1	4		2		1							
Ro4			1	1				1	1		1	2			1	1				4	4				
Ro5	1		2	4	6					2		2	2	12	1	9		1		5	6				
Ro6			5	1	9	8		6	2	2		3	10	1	15	8	2	1		9	2				
Ro7	4		13	2	10	2	3	4		3	7	3	2	1	6	5	7	2		3	4	2			
Ro8					2			1										3				1			
Trapeziform cubic																									
Tra1	5		1	5	4	1			2	2	7		3	1		1	1								
Bilobate																									
Bi1	5		12	22	19	3	5	10	12	10	2	9	13	24	7	35	17	16		8	22				
Bi2	23		8	9	3	23	10	7	19	24	10	36	16	36	13	3	7	12		18	13				
Bi3													2			1		1							
Bi4			2					2				1	2												
Bi5													1					3		2					
Bi6							2					3													
Bi7	15		8	11	9	12	21	28	20	20	16	22	7	15	11	12	8	7			14				
Bi8	9		40	10	25	27	9	10		23	22	4	25	4	13	8	14	4		22	32	2			
Bi9	19			18	9	7	26		18	11	7	1	6				1	2		15					
Bi10	10		1	3	16		22	5		2	11		1	4	10	10	3				2				
Bi11	12		6	13	5	17	8		7	2	5	8	9	16	4	8	5	4		5	15	3			
Bi12	8			12	7		2	5	3		2	2	2		5		3	3		3					
Bi13				1			2		6																
Bi14	12		14	2	5	24	27	2	12	10	5	9	4	18	39	11	30	10		8	6				
Bi15																									
Crosses																									
Cr1				9			2	7					4												
Cr2	13		9	1	10	10	21	6	58	37	36	21	9	26	27	17	35	23		1	16				
Cr3			7			24	7	1	12	5	3	1	12	6		3	1			5					
Cr4			5		5		1			2	2	4	4	3	1	3		4							
Cr5	20		13	30	22	14	36	54	16	15	25	31	12	9	14	20	14	4		30	10				
Cr6	1				9	12	7	1	1	2		3		4	5	2	8	10		7	14				
Cr7	1		4		2	3	2	5	6		5	5	1	4		5		3		4					
Cr8	3		4	1		1				2			3					1							
Polylobate																									
Poly1			2			1	2			4	3			1		1				3					

Table S1

ID samples, BOL	5a	6p	8n	9e	10b	11a	12l	13e	17a	17h	19a	21a	21j	22a	24n	25a	25j	26a	27n	28a	30j	32a	32e	35a	35e
Poly2																					2				
Poly3	2		7		2	1	3	9			5		4	2		6	3	1							
Poly4	1			2			1		5		2			3			1								
Saddle																									
S1	5				4			5	3	3	3	5	12	5	10	18	5	4		7					
S2	1		1						2	5	1	4	7		3		1	4		1	1				
S3			8		2	4		2		2	3	4		2	7	1	3			1	4				
S4	3		8	2	6	1		3	3	4	16		13	22	1	4	5	6			8	1			
S5	18		7				2	5		2		5				2	7	6		8	5				
Other phytolith types																									
Acicular																									
Aci1	11		7	16	2	100	59	6	59	6	8	31	9	10	16	12	3	1			4				
Aci2																									
Aci3																									
Blocky																									
Blo1			6	30	14			1													2				
Blo2																									
Blo3, Blo6 or Blo7	14		19	52	55	279	257	15	266	29	12	114	13	31	51			3		100	7	7			
Blo4 or Blo5	16		24	49	46	598	172	16	302	24	2	45	5	15	48	8	10			132	11	4			
Blo8	1		1													3	1			5					
Blo9										1		2		2											
Blo10													2							1					
Elongate																									
El1					4																				
El2			1					5					1				2								
El3	40		4	114	70	328	288	6	184	43	42	110	22	69	94	10	85	22		22	53	4			
El4																									
El5				3																					
El6																									
Epidermal silicified structures																									
Str1																									
Str2																									
Sto1						2																			
Trac1			1					2					3			1									
Globular																									
Glo1	2			1	1			2	3	1	2	12	17	3	22	2	2	2			39				
Glo2	11			4	21	3	1	4	7	4		20	13	6	15		9	2			2	3			
Glo3																									
Glo4																									
Glo5	7			11	4				1		1			2	3		4				1				

Table S1

ID samples, BOL	5a	6p	8n	9e	10b	11a	12l	13e	17a	17h	19a	21a	21j	22a	24n	25a	25j	26a	27n	28a	30j	32a	32e	35a	35e
Glo6																									
Glo7																									
Glo8																						1			
Polyhedral body																									
Pol1			1																						
Polyhedral plate																									
Pla1																									
Pla2					7																				
Pla3								1	2		2					1									
Pla4						2	1		1			3	4		4										
Pla5	1			1							1				2										
Pla6																									
Pla7																									
Pla8																									
Pla9			1					2					1				3								
Undescriptible			1			2		3		1			9			11									
Sum total	**303**	**S**	**285**	**454**	**424**	**1596**	**1002**	**265**	**1035**	**349**	**307**	**533**	**305**	**380**	**466**	**255**	**323**	**173**	**S**	**463**	**311**	**28**	**S**	**S**	**S**
Sum GSSCs	**200**	**-**	**219**	**173**	**200**	**282**	**224**	**202**	**210**	**240**	**237**	**196**	**206**	**242**	**211**	**207**	**204**	**143**	**-**	**203**	**192**	**9**	**-**	**-**	**-**

Table S2

BOL, 25j						Plant Functional Types									Biomes						
Family	**Pollen taxa**	**Plant habit**	**Pollen count**	**Pollen %**	**Sqrt %**	**wte**	**te**	**tr1**	**tr2**	**tr3**	**sf**	**df**	**g**	**aq**	**WAM F (wte)**	**TRFO (te)**	**TSFO (tr1)**	**TDFO (tr2)**	**SAVA (tr3+g)**	**STEP (sf+g)**	**DESE (df+g)**
Amaranthaceae	*Celosia trigyna**	Herb	5	0.6	0.79	1		1	1	1	1				0.79	0.00	0.79	0.79	0.79	0.79	0.00
Asteraceae	Asteraceae echinate*	NC	7	0.9	0.93	1		1	1	1	1	1			0.93	0.00	0.93	0.93	0.93	0.93	0.93
Chenopodiaceae	cf. *Atriplex*	Herb	8	1.0	1.00										0.00	0.00	0.00	0.00	0.00	1.00	1.00
Combretaceae	*Combretum* molle*	Tree/Shrub	9	1.1	1.06				1	1					0.00	0.00	0.00	1.06	1.06	0.00	0.00
Cyperaceae	Cyperaceae	Herb	125	15.6	3.95	1	1	1	1	1	1	1		1	3.95	3.95	3.95	3.95	3.95	3.95	3.95
Euphorbiaceae	*Acalypha*	NC	2	0.2	0.50	1	1	1	1	1	1				0.50	0.50	0.50	0.50	0.50	0.50	0.00
Euphorbiaceae	*Alchornea*	Tree/Shrub	21	2.6	1.62	1		1	1						1.62	0.00	1.62	1.62	0.00	0.00	0.00
Euphorbiaceae	*Tetrorchidium*	Tree/Shrub	1	0.1	0.35			1							0.00	0.00	0.35	0.00	0.00	0.00	0.00
Fabaceae	Fabaceae	NC	1	0.1	0.35	1	1	1	1	1	1				0.35	0.35	0.35	0.35	0.35	0.35	0.00
Hymenocardiaceae	*Hymenocardia*	Tree/Shrub	2	0.2	0.50			1	1	1					0.00	0.00	0.50	0.50	0.50	0.00	0.00
Mimosaceae	*Acacia** Group I	Tree/Shrub	3	0.4	0.61			1	1	1	1				0.00	0.00	0.61	0.61	0.61	0.61	0.00
Mimosaceae	*Albizia**	Tree	1	0.1	0.35	1	1	1	1	1					0.35	0.35	0.35	0.35	0.35	0.00	0.00
Mimosaceae	*Mimosa pigra**	Herb/Shrub	1	0.1	0.35				1	1	1			1	0.00	0.00	0.00	0.35	0.35	0.35	0.00
Mimosaceae	*Prosopis africana*	Tree/Shrub	3	0.4	0.61		1	1	1	1	1				0.00	0.61	0.61	0.61	0.61	0.61	0.00
Myricaceae	*Myrica*	Tree/Shrub	1	0.1	0.35	1									0.35	0.00	0.00	0.00	0.00	0.00	0.00
Myrsinaceae	cf. *Embelia**	Tree/Shrub	2	0.2	0.50	1									0.50	0.00	0.00	0.00	0.00	0.00	0.00
Myrsinaceae	*Maesa lanceolata**	Tree	1	0.1	0.35	1		1	1	1					0.35	0.00	0.35	0.35	0.35	0.00	0.00
Myrsinaceae	*Rapanea melanophloeos*	Tree	1	0.1	0.35	1									0.35	0.00	0.00	0.00	0.00	0.00	0.00
Myrtaceae	*Syzygium* guineense*	Tree	1	0.1	0.35	1	1	1	1	1					0.35	0.35	0.35	0.35	0.35	0.00	0.00
Oleaceae	*Olea capensis*	Tree	28	3.5	1.87	1									1.87	0.00	0.00	0.00	0.00	0.00	0.00
Poaceae	Poaceae	Herb	549	68.4	8.27								1	1	0.00	0.00	0.00	0.00	8.27	8.27	8.27
Potamogetonaceae	*Potamogeton thunbergii*	Herb aquatic	1	0.1	0.35									1	0.00	0.00	0.00	0.00	0.00	0.00	0.00
Pteridophyte	Monolete spore, psilate	Fern	1	0.1	0.35	1	1	1	1					1	0.35	0.35	0.35	0.35	0.00	0.00	0.00
Pteridophyte	Polypodiaceae, monolete	Fern	1	0.1	0.35	1	1	1	1						0.35	0.35	0.35	0.35	0.00	0.00	0.00
Pteridophyte	*Pteridium* aquilinum*	Fern	1	0.1	0.35	1	1	1	1						0.35	0.35	0.35	0.35	0.00	0.00	0.00
Pteridophyte	Trilete spore, foveolate	Fern	1	0.1	0.35	1	1	1	1	1					0.35	0.35	0.35	0.35	0.35	0.00	0.00
Rhamnaceae	Rhamnaceae undiff.	Tree/Shrub/Liana	3	0.4	0.8	1		1	1	1	1				0.78	0.00	0.78	0.78	0.78	0.78	0.00
Rubiaceae	*Psychotria**	Tree/Shrub	1	0.1	0.35	1		1	1	1					0.35	0.00	0.35	0.35	0.35	0.00	0.00
Scrophulariaceae	*Stemodia* serrata*	Herb	3	0.4	0.61			1	1	1	1				0.00	0.00	0.61	0.61	0.61	0.61	0.00
Tiliaceae	*Triumphetta**	Herb or Shrub	1	0.1	0.35	1	1	1	1	1	1				0.35	0.35	0.35	0.35	0.35	0.35	0.00
Typhaceae	*Typha*	Herb aquatic	1	0.1	0.35									1	0.00	0.00	0.00	0.00	0.00	0.00	0.00
Ulmaceae	*Celtis*	Tree	1	0.1	0.35	1	1	1	1	1					0.35	0.35	0.35	0.35	0.35	0.00	0.00
Zygophyllaceae	*Zygophyllum**	Herb or Shrub	7	0.9	0.93						1				0.00	0.00	0.00	0.00	0.00	0.93	0.00
Unidentified	Unidentified	NC	9	1.1	2.5																
	TOTAL		803	100.0	33.07					***TOTAL Biome score =***					**15.5**	**8.2**	**15.1**	**16.2**	**21.8**	**20.0**	**14.1**
	Unidentifiable		39																		

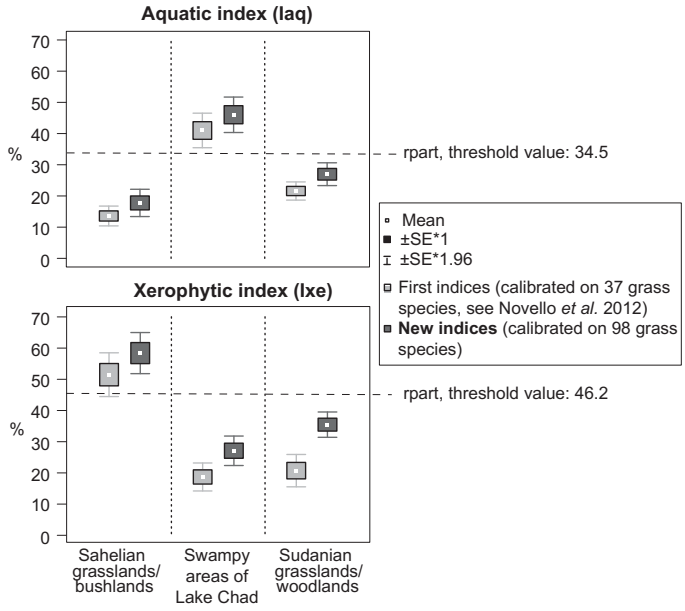

Figure S1 Comparison between the first and new grass phytolith indices calculated for ten modern mud samples from Lake Chad, 18 modern soil/mud samples from the Sahelian domain of Chad, and 29 modern soil/mud samples from the Sudanian domain of Chad. Modern phytolith soil assemblages are compiled from Novello et al. (2012) and from new unpublished data. Complementary ANOVA tests indicate significant differences between groups with the three indices (p<0.01).